Cerebral Cortex November 2007;17:2675–2695
doi:10.1093/cercor/bhl177
Advance Access publication January 30, 2007

Optical Imaging of Contrast Response in Macaque Monkey V1 and V2

Haidong D. Lu and Anna W. Roe

Department of Psychology, Vanderbilt University, Nashville, TN, USA

Our studies on brightness information processing in Macaque monkey visual cortex suggest that the thin stripes in the secondary visual area (V2) are preferentially activated by brightness stimuli (such as full field luminance modulation and illusory edge-induced brightness modulation). To further examine this possibility, we used intrinsic signal optical imaging to examine contrast response of different functional domains in primary and secondary visual areas (V1 and V2). Color and orientation stimuli were used to map functional domains in V1 (color domains, orientation domains) and V2 (thin stripes, thick/pale stripes). To examine contrast response, sinusoidal gratings at different contrasts and spatial frequencies were presented. We find that, consistent with previous studies, the optical signal increased systematically with contrast level. Unlike single-unit responses, optical signals for both color domains and orientation domains in V1 exhibit linear contrast response functions, thereby providing a large dynamic range for V1 contrast response. In contrast to domains in V1, domains in V2 exhibit nonlinear responses, characterized by high gain at low contrasts, saturating at a mid–high contrast levels. At high contrasts, thin stripes exhibit increasing response, whereas thick/pale stripes saturate, consistent with a strong parvocellular input to thin stripes. These findings suggest that, with respect to contrast encoding, thin stripes have a larger dynamic range than thick/pale stripes and further support a role for thin stripes in processing of brightness information.

Keywords: color domains, contrast, functional organization, optical imaging, orientation domains, thin stripes, V1/V2

Introduction

Contrast response is one of the most important properties of visual neurons. It has been shown that individual visual neurons encode contrast differently with respect to gain, saturation, and threshold. In primates, magnocellular (M) and parvocellular (P) neurons in the lateral geniculate nucleus (LGN) are characterized by distinct contrast response signatures (Kaplan and Shapley 1982). Magnocellular neurons have higher contrast sensitivity and higher contrast gain than parvocellular neurons. In fact, at contrasts lower than around 10%, parvocellular neurons are unresponsive. Magnocellular neurons exhibit contrast gain control, whereas parvocellular neurons respond to contrast in a relatively linear fashion. Koniocellular neurons are a heterogeneous population of neurons and have a broad range of contrast response functions (CRFs) (Norton et al. 1988; Hendry and Reid 2000; Solomon et al. 2002).

Efforts to track the M/P trail through specific visual cortical structures (such as blobs and interblobs in primary visual area [V1] and thin, pale, and thick stripes in secondary visual area [V2] of the primate) have led to hotly debated viewpoints. Although M and P inputs to V1 are clearly segregated in layers 4Cα and 4Cβ, respectively, from there, opinions diverge. In V1, some studies suggest there is a higher contrast sensitivity in the blobs (Hubel and Livingstone 1990; Edwards et al. 1995), perhaps due to a predominance of M input to the blobs (Blasdel et al. 1985; Tootell et al. 1988b; Lachica et al. 1992; Yabuta and Callaway 1998). However, others emphasize the presence of mixed M and P influences in both blobs and interblobs of V1 (Nealey and Maunsell 1994). In a study that focused on distance from blob centers (Edwards et al. 1995), cells in blobs were found to exhibit lower spatial frequency response and higher contrast sensitivity than their interblob counterparts. Consistent with previous reports (Lennie et al. 1990), Edwards et al. found no bimodal distribution, but rather a gradual shift in the population response with distance from blob center. There are also direct inputs to the blobs from blue-on koniocellular neurons in the middle K layers (Hendry and Calkins 1998), some of which exhibit linear parvo-like CRFs (Solomon et al. 2002). Blue-off inputs appear to terminate slightly deeper in layer 4A (Chatterjee and Callaway 2003).

With respect to functional compartments in V2, the expectation was that thick stripes, believed to be dominated by M inputs, should exhibit higher contrast sensitivity. However, in principle, magnocellular and parvocellular inputs reach all the stripe compartments in V2. The thin stripes receive both M and P input primarily by way of the blobs and thick and pale via the interblob columns (Livingstone and Hubel 1984a, 1984b, 1987; Sincich and Horton 2002). Levitt et al. (1994) found that thick stripes did have the highest contrast sensitivity values, although semisaturation values showed no significant difference between thin, pale, and thick stripes. Overall, they found surprisingly little quantitative differences between thin, pale, and thick stripes and argued on the side of homogeneity. The 2-deoxyglucose methodology revealed that low-contrast (8%) achromatic gratings produced faint labeling in both thin and thick, but not pale, stripes (Fig. 16 in Tootell and Hamilton 1989). This suggests M contribution could also be prominent in the thin stripes. K inputs to V2 could arrive via the blobs and layer 4A in V1 or directly from the koniocellular neurons in the LGN. However, given the heterogeneity of K inputs and their relatively weak response to achromatic gratings (compared with M and P), their contribution to V2 contrast response may be weaker.

In most single-unit studies, stimuli are tailored to the preferences of individual neurons. However, under natural viewing conditions, entire neural structures are challenged with single stimuli. Thus, studying cortical responses at the population level

is also crucial for understanding the organization and flow of sensory information. Using single stimulus to study responses simultaneously in multiple cortical areas is a useful way to differentiate areal roles in sensory processing. Indeed, this single stimulus/multiarea approach, one which is commonly used in functional magnetic resonance imaging studies (e.g., Dumoulin et al. 2003), has been used in a number of optical imaging studies to examine both visual (e.g., Xu et al. 2004; Roe et al. 2005a, 2005b; Schmidt and Lowel 2006; Zhan and Baker 2006) and other sensory (Chen and Kaplan 2003; Kalatsky et al. 2005) cortical processing. Optical imaging of intrinsic signals also provides other advantages. It has sufficiently high spatial resolution (~100 μm) to map responses of cortical functional structures such as orientation domains, blobs, and stripes. It can be used to map relatively large regions (e.g., millimeters) of cortex and provide a good understanding of overall functional architecture. Importantly, imaged reflectance signals provide an additional quantitative approach for measuring neural response.

In this paper, we use the optical imaging approach to compare contrast response in V1 and V2 of primate visual cortex (cf., Tootell et al. 1988b; cf., in cat, Carandini and Sengpiel 2004; Zhan et al. 2005). We have measured the CRFs of color and orientation domains within relatively large fields of view of V1 and V2. Our findings show that, as measured with optical imaging, the population contrast response of V1 (both blobs and interblobs) tends to be linear, whereas that in V2 tends to be nonlinear. Furthermore, the contrast response of thin stripes in V2, distinct from that of thick and pale stripes in V2, is consistent with its role in brightness processing.

Methods

Animal Preparation

Three Macaque monkeys (*Macaca fascicularis*) were anesthetized (thiopental sodium, 1–2 mg/kg/h intravenously [i.v.] and isoflurane, 0.2–1.5%), paralyzed with vecuronium bromide (0.05 mg/kg/h i.v.), and artificially ventilated. Anesthetic depth was assessed continuously via implanted wire electroencephalographic electrodes, end-tidal CO_2, oximetry, heart rate, and by regular testing for response to toe pinch while monitoring heart rate changes. Eyes were dilated (atropine sulfate) and fitted with contact lenses of appropriate curvature (Danker Laboratories Inc., Sarasota, FL) to focus on a computer screen. Eyes were aligned by converging the receptive fields (RFs) of a binocular V1 neuron with a Risley prism over one eye. Alignment was checked before and after each recording. Craniotomy and durotomy were performed to expose visual areas V1 and V2 (near the lunate sulcus at an eccentricity of 3–6 deg from the fovea). In one case, a chronic chamber was implanted. All surgical and experimental procedures conformed to the guidelines of the National Institutes of Health and were approved by the Vanderbilt Animal Care and Use Committees.

Visual Stimulus

Full-screen drifting sine-wave gratings were created using custom-made computer programs (STIM, Kaare Christian or in Matlab, Dan Shima) and presented on a CRT monitor (Barco Calibrator PCD-321, Kuurne, Belgium). The stimulus screen was gamma corrected using (Minolta Chroma Meter CS-100, Ramsey, NJ) photometer and positioned 38 inches from the eyes. Screen extent spanned 24 × 18 deg of visual field. Mean luminance for all stimuli, including the blank stimulus (uniform gray screen), was kept at 30 cd/m^2. In some stimulus conditions, electromechanical shutters were placed in front of the eyes for monocular stimulation.

Stimuli for Revealing Functional Maps

1) High-contrast black and white (BW) sinusoidal gratings (typically 1.5 c/deg drifted at 2 Hz) presented at 1 of 4 orientations (0°, 45°, 90°, and 135°) presented to either eye randomly. These maps were appropriately summed to reveal ocular dominance (OD) and orientation maps. 2) To reveal color domains, we used isoluminant red–green (RG) (0° or 90°) gratings of the same spatial (0.15 c/deg for cases 1, 2, and 3 and 0.5 c/deg for cases 4 and 5) and temporal frequencies (0.5–1 Hz) and mean luminance (30 cd/m^2) as the BW gratings. RG gratings were generated by modulating red and green guns in counterphase so that red increase was accompanied by green decrease. Because the peak luminance values for red and green were set to be equal, the stimulus is isoluminant and only the color is modulated (100% contrast for both red and green guns). Red Commision Internationale de L'Eclairage (CIE) values are 0.302 and 0.545; green CIE values are 0.593 and 0.340. Thus, for color domain mapping, in addition to a blank condition (mean luminance 30 cd/m^2), 4 different gratings (RG horizontal, RG vertical, BW horizontal, BW vertical) were presented to the left eye and to the right eye, resulting in 9 different randomly interleaved stimulus conditions.

Luminance Contrast Stimuli

To test cortical responses to different luminance contrasts, BW drifting luminance gratings of different contrast were presented binocularly to the animal. Based on previous single-unit studies (Levitt et al. 1994; Edwards et al. 1995), 6 different spatial frequencies were chosen (0.21, 0.42, 0.84, 1.68, 3.36, and 6.72 c/deg). In 2 of the cases, the temporal frequencies of the sine-wave gratings were fixed at 2 and 5 c/s, and in the other 2 cases, the speed were fixed at 4.5 deg/s. For each spatial frequency, 2 orientations (0° and 90°) and 5 levels of contrast (0, 0.1, 0.2, 0.4, and 0.8, Michelson contrast) were presented in a random order. Mean luminance for all stimuli, including blank (uniform gray screen), was kept at 30 cd/m^2.

Optical Imaging

In one case, an optical chamber was mounted to the skull, filled with silicone oil, and sealed with a glass window. In the other cases, the brain was stabilized with agar and images were obtained through a glass coverslip. Images of reflectance change (intrinsic hemodynamic signals) corresponding to local cortical activity were acquired using either Imager 2001 or Imager 3001 (Optical Imaging Inc., Germantown, NY) with 630-nm illumination (for details, see Roe and Ts'o 1995; Ramsden et al. 2001). Signal-to-noise ratio was enhanced by trial averaging (25 trials per stimulus condition) and by synchronization of acquisition with heart rate and respiration. Each stimulus was presented for 4 s, during which 20 consecutive image frames were taken (5 Hz frame rate). Interstimulus interval for all stimuli was at least 8 s. For the Imager 2001 system, each frame had 372 × 240 pixels and represented 8 × 6 mm of cortex. For the Imager 3001 system, frame size was 504 × 504 pixels and represented 8 × 8 mm cortex. Stimuli were presented in blocks. Each block contained 8 grating stimuli (2 orientations and 4 levels of contrast) and a blank. All stimuli were presented in a randomly interleaved fashion. Stimulus onset occurred after the first frame.

Data Analysis

Single-Condition Maps

For each stimulus condition, we constructed a "single-condition map." The gray value of each pixel in the "single-condition map" represents the percent change of the light reflectance signal after the stimulus was presented. Specifically, the gray value of each pixel was calculated using the following function:

$$\Delta R/R = (F_{5\text{-}20} - F_1)/F_1,$$

in which $\Delta R/R$ represents percent change, $F_{5\text{-}20}$ is the average raw reflectance values of frames 5–20 (1–4 s after stimulus onset). F_1 is the raw reflectance value of the first frame (taken before stimulus onset and thus represents the baseline activity). Single-condition maps obtained in this way represent the percent intrinsic signal changes compared with the initial (prestimulus) baseline condition. This is usually a negative value (–0.01 ~ –0.2%). These maps were further used for calculating differential maps and for quantification. For constructing domain masks, additional high-pass or low-pass filtering was applied (see below). These are the only places filtering was performed.

Constructing Domain Masks

To examine contrast response of different functional domains within V1 and V2, we generated domain masks based on "difference maps," which is a subtraction of a pair of "single-condition maps" (e.g., horizontal gratings minus vertical gratings, color gratings minus luminance gratings). Pixel values in "difference maps" represent the preference of each pixel to either one of the 2 stimuli. To identify regions of maximal response, difference maps were first smoothed (Gaussian filter, 8 pixel kernel). Low-frequency noise was reduced by convolving the maps with a 150-pixel diameter circular mean filter and subtracting the result from the smoothed maps. The result maps were thresholded at the top 10% pixels for color domains or 20% pixels for orientation domains (Chen et al. 2001; Ramsden et al. 2001).

A total of 6 functional domain masks were created for each case. These 6 functional masks were used for all contrast conditions in that case. Among these masks, "V1 horizontal," "V1 vertical," "V2 horizontal," and "V2 vertical" were obtained from horizontal–vertical (HV) difference map in responding to optimal spatial and temporal frequencies (e.g., Fig. 2*A*); "V1 color domain" and "V2 thin stripe" masks were based on preferential response to isoluminant RG gratings (see Fig. 2*B*). For calculation of response within color domains and for thin stripes, the responses to horizontal and vertical gratings at each pixel within the mask were simply averaged (because color domains and thin stripes are not orientation selective, these values were very similar). For orientation domains, because there were no significant differences between the response of horizontal domains to horizontal gratings and vertical domains to vertical gratings, contrast responses in each domain type to the preferred orientations were combined (i.e., optimal responses were combined). Consistent with previous studies (Ts'o et al. 1990; Malach et al. 1994; Roe and Ts'o 1995; Xu et al. 2004), orientation maps appeared continuous across the borders of pale and thick stripes.

A blood vessel map was also created based on an image of the cortex obtained with 570 nm (green) illumination; pixels within the major blood vessel regions were excluded from analysis. Therefore, all subsequent quantification was done on vessel-free zones. In this study, we did not differentiate between thick and pale stripes.

Alternative Masking Method

To examine the robustness of our results, we also took measurements using an alternative masking method. We constructed domain masks by selecting circular regions (80, 160, 240 μm for V1 color domain and orientation domains; 160, 320, 480 μm for V2 thin stripe and thick/pale domains) centered on domain centers (maximum reflectance change) in each of the orientation and color maps. The choice of larger domain sizes for V2 is based on the observation that these V2 domains are at least 2 times larger than V1 domains (Roe and Ts'o 1995; Ramsden et al. 2001; Ts'o et al. 2001; Xu et al. 2004).

Quantification of Contrast Response

Contrast responses were obtained from single-condition maps by averaging the values of pixels falling within the same type of domains, so the values of contrast response is in the unit of percent change ($\Delta R/R$). Those 6 domain masks were applied to each of the 30 single-condition maps (30 grating stimuli presented at 5 contrasts and 6 spatial frequencies). For each single-condition map and domain mask pair, one single average value was obtained. For example, to obtain the average domain response value to 0.1 contrast horizontal grating, we did the following: 1) A single-condition map response to 0.1 contrast horizontal gratings (averaged over trials) was generated, which is a 504 × 504 matrix of percent change values. 2) The average pixel values per domain were obtained, resulting n values (n is the number of horizontal domains in horizontal domain mask). 3) The mean and standard deviation (SD) of all the domain values to this particular stimulus were calculated. This procedure was conducted for each of the 6 domain masks and each of the 30 contrast maps obtained.

Results

A total of 4 contrast imaging experiments were performed on 4 hemispheres of 3 adult macaque monkeys. In each experiment, we collected maps that revealed functional organization of OD, orientation, and color domains. We collected maps of contrast response at 5 contrast levels, 6 spatial frequencies (4 spatial frequencies in one case), and 2 orientations. Each map was a sum of at least 25 trials per condition. To make valid quantitative comparisons, the preparation had to be very stable for the entire imaging session. In several cases that are not presented here, a change of physiological baseline in our imaging session rendered the data set incomplete. We have obtained 4 cases with reasonably good stable results. All 4 cases revealed qualitatively similar results. In this paper, we have illustrated in detail optical imaging and quantitative data analysis from 3 cases, one illustrating both V1 and V2, another illustrating V1, and another illustrating V2. The remaining case provided qualitatively similar results, but not all maps were of sufficient quality to perform quantitative analysis.

Functional Domains in V1 and V2

Figure 1 shows 4 optical images from one case; the imaging area is 8 × 8 mm. Figure 1*A* is the blood vessel pattern obtained with illumination of 570 nm (green) light. The lunate sulcus is located at the top of the image. Figure 1*B–D* are difference maps obtained by subtracting 2 single-condition maps. Figure 1*B* is the OD map (left eye – right eye); dark regions indicate locations preferentially activated by the left eye stimulus, and white regions are those preferentially activated by the right eye. It clearly shows alternating OD stripes in V1 but not in V2, thereby delineating the V1/V2 border (indicated by a short line at right). Orientation structures are shown in Figure 1*C* (HV); dark regions represent areas preferentially responsive to horizontal stimuli, and light regions are those preferentially responsive to vertical stimuli. Both V1 and V2 have strongly activated orientation maps; V2 orientation domains (arrowheads) are characteristically larger than those in V1 and are separated by zones of poor orientation selectivity (arrows) (Peterhans and von der Heydt 1993; Malach et al. 1994; Roe and Ts'o 1995; Ts'o et al. 2001; Xu et al. 2004).

Figure 1*D* is the color map obtained by subtracting stimulation with isoluminant RG color gratings and luminance contrast gratings. Because color and luminance gratings contained the same spatial frequency (0.15–0.5 c/deg), temporal frequency (0.5–1 Hz), and average luminance (30 cd/m^2), the only difference between these 2 stimuli is the color content of the stimulus. We considered the possibility that there remained a small luminance contrast difference in the RG stimuli. However, our examination of high-contrast minus low-contrast stimuli never revealed any structured maps and never any blob-like pattern. Thus, we attribute the differences in activation shown in Figure 1*D* to preferential color response. Dark regions in these maps are areas that have stronger response to color stimuli (or weaker response to luminance stimuli) in comparison with the other regions. In V1, the color map has a striking "blob-like" pattern that has been shown to have a high-degree overlap with cytochrome oxidase (CO) blobs (Landisman and Ts'o 2002a). In V2, the location of the color domains (indicated by arrows in *C* and *D*) colocalizes with regions of poor orientation organization (arrows in *C* and *D*) and is complementary to regions of strong orientation response in V2 (arrowheads in *C* and *D*).

In this case, functional domain outlines were obtained with thresholding method. Figure 2*A* shows the horizontal orientation mask (blue) and vertical orientation mask (green) overlaid on the orientation map. Figure 2*B* shows the color domain mask

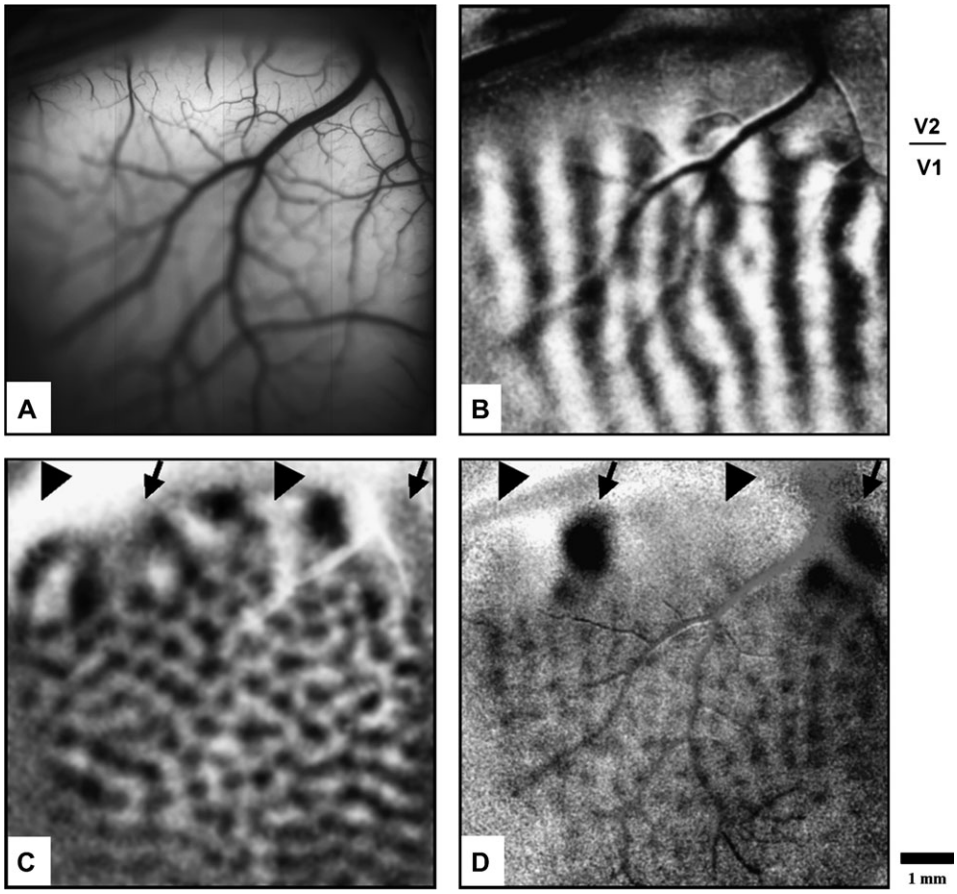

Figure 1. Optical images of functional domains in Macaque V1 and V2. (*A*) Blood vessel map obtained by using green light (570 nm). Lunate sulcus is located at the top. (*B*) OD map (left eye minus right eye). V1/V2 border (indicated by short line at right) is demarcated by the lack of ocular columns in V2. (*C*) Orientation preference map (horizontal minus vertical). V2 orientation domains (indicated by arrowheads) are up to several times larger than those of V1. They are complementary to locations of thin stripes (indicated by arrows). (*D*) Color map (RG isoluminant gratings minus luminance gratings) in which V2 thin stripes (indicated by arrows) and V1 color domains are more activated by the color grating than luminance grating stimuli. Scale bar: 1 mm, applies to (*A–D*).

(red) overlaid on the color map. In Figure 2*C*, the color domains are overlaid on the orientation map, illustrating that the color domains (which are regions of low orientation selectivity) typically do not coincide with centers of orientation-selective domains. Figure 2*D* shows both orientation masks and the color mask superimposed on a single blood vessel map. This overlay illustrates that orientation and color domains have minimal overlap (cf., Bartfeld and Grinvald 1992; Landisman and Ts'o 2002a).

Contrast Response Signals

Figure 3 illustrates that stimuli of different contrast elicit different magnitudes of intrinsic signal reflectance change in V1. Shown are signals from vertical orientation domains in response to either vertical (blue) or horizontal (red) grating stimuli. Each trace is the average of 68 domains in response to a particular grating contrast (0.1, 0.2, 0.4, or 0.8, color code indicated at right). Typical of intrinsic cortical signals, the signal takes 2–3 s to peak and is on the order of 0.1% in amplitude. Clearly, higher contrast stimuli lead to larger reflectance changes. The blank condition elicits a relatively flat time course (black trace, the small negative drift may come from noise). Moreover, as expected, optimal stimuli (e.g., vertical, blue) produce activations of slightly greater amplitude than non-optimal stimuli (e.g., horizontal, red), thereby leading to the differential response typically observed in orientation maps.

Contrast Response: General Activity

To measure contrast response, we first generated a series of contrast response maps. Cortical contrast response was measured from single-condition maps, that is, percent change from prestimulation reflectance level. As expected, in general, response amplitude increased monotonically with contrast. Figure 4 shows cortical responses to 30 different gratings (response to horizontal and vertical gratings were averaged, see Supplementary Figs 1–3 for response to horizontal and vertical alone), each presented at a different contrast (0, 0.1, 0.2, 0.4, and 0.8) and spatial frequency (0.21, 0.42 0.84, 1.68, 3.36, and 6.72 c/deg). In each single-condition map, dark pixels indicate greater responses and bright pixels indicate less response. All images were clipped at –0.2% to 0.1% (i.e., reflectance change lower than –0.2% has same gray level as –0.2%, and reflectance higher than 0.1% is set at same gray level as 0.1%). With qualitative inspection, it is apparent that for a single spatial frequency (except perhaps 6.72 c/deg, top rows of Fig. 4), the response increases with contrast (i.e., image becomes darker on average with increasing the contrast). This occurs within both V1 and V2 (also see Supplementary Fig. 3 for color-coded version). The contrast responses of images

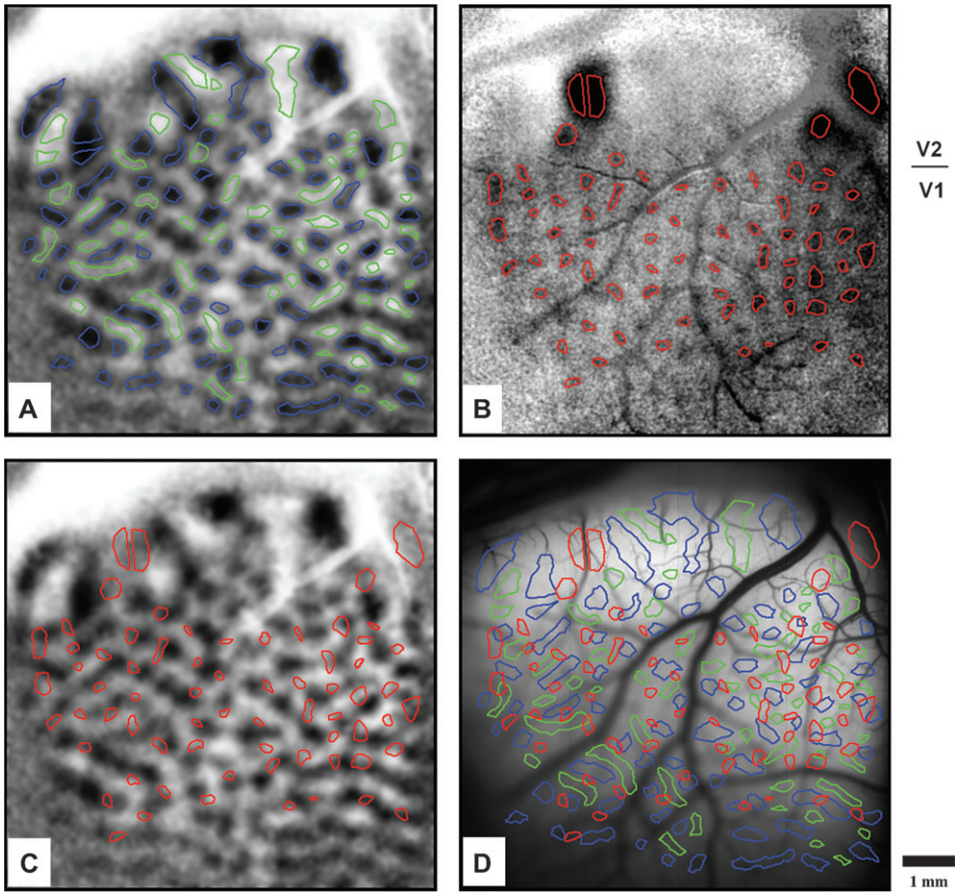

Figure 2. Functional domain masks. All figures are from Figure 1. (*A*) Horizontal (blue) and vertical (green) orientation masks overlaid on the HV orientation map. (*B*) Color domain mask (red) overlaid on the color—luminance map identifies color domains in V1 and thin stripes in V2. (*C*) Color domain mask (red) overlaid on the HV orientation map. (*D*) Orientation domain masks and color domain mask overlaid on blood vessel map. There is little overlap between orientation and color domains. Scale bar: 1 mm, applies to (*A*–*D*).

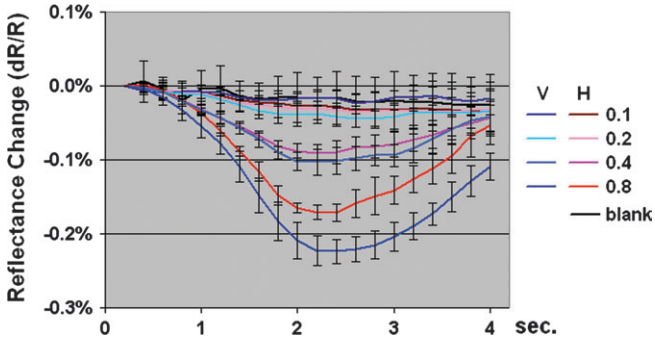

Figure 3. Intrinsic signal time courses of vertical orientation domains in V1 in response to 8 gratings with different contrast and orientation and 1 blank. The first frame (first 0.25 s) is used as a reference frame and was subtracted out from the rest of the frames. Imaging frequency 5 frames per second. Stimulus conditions are indicated in legend: H, horizontal; V, vertical. Numbers indicate contrast level. Spatial frequency of the stimulus: 1.68 c/deg. Error bar: SD over vertical domain population.

obtained in response to horizontal and vertical gratings were very similar (see Supplementary Figs 1 and 2).

Examination of the images from Figure 4 reveals that the overall activation level from V1 is stronger than that from V2 (more dark pixels in V1), indicating that, in the anesthetized monkey, the imaged response to sinusoidal gratings, presented at these spatiotemporal frequencies, in V1 is consistently stronger than that in V2. To quantify this difference in general responsiveness, we plotted the pixel distributions of reflectance values in V1 and V2. Pixels falling within V1 and V2 (Fig. 5 top inset) were determined by imaging for OD. Figure 5 illustrates the relative pixel distributions from the best spatial frequency (1.68 c/deg). With increasing contrast (top to bottom graphs), the average reflectance change (means indicated by arrows) increases for both V1 and V2. At lower contrasts (blank, 0.1, 0.2), V1 and V2 exhibit no significant difference. However, at the higher contrasts (0.4, 0.8), imaged response in V1 is stronger than that in V2.

This difference is most apparent at optimal spatial frequencies. For high-contrast (0.8) gratings at preferred spatial frequencies (0.42, 0.84, and 1.68 c/deg), the average percent change in V1 is 46%, 67%, and 80% higher than that from V2, respectively (*t*-tests, $P = 0.04$, 0.02, 0.00004). For nonpreferred spatial frequencies (0.21, 3.36, 6.72 c/deg), although the overall percent change is also higher (40–100%) in V1 than in V2, the difference between V1 and V2 is not significant (*t*-test, $P = 0.14$, 0.16, 0.5) due to the lower signal/noise ratio at these spatial frequencies. Thus, at higher contrasts and within the preferred spatial frequency range, average response in V1 is stronger than that in V2 (under anesthetized experimental conditions).

Figure 6 illustrates both functional maps and single-condition contrast response maps (sum of horizontal and vertical single conditions) from another case. In this case, only V1 is available

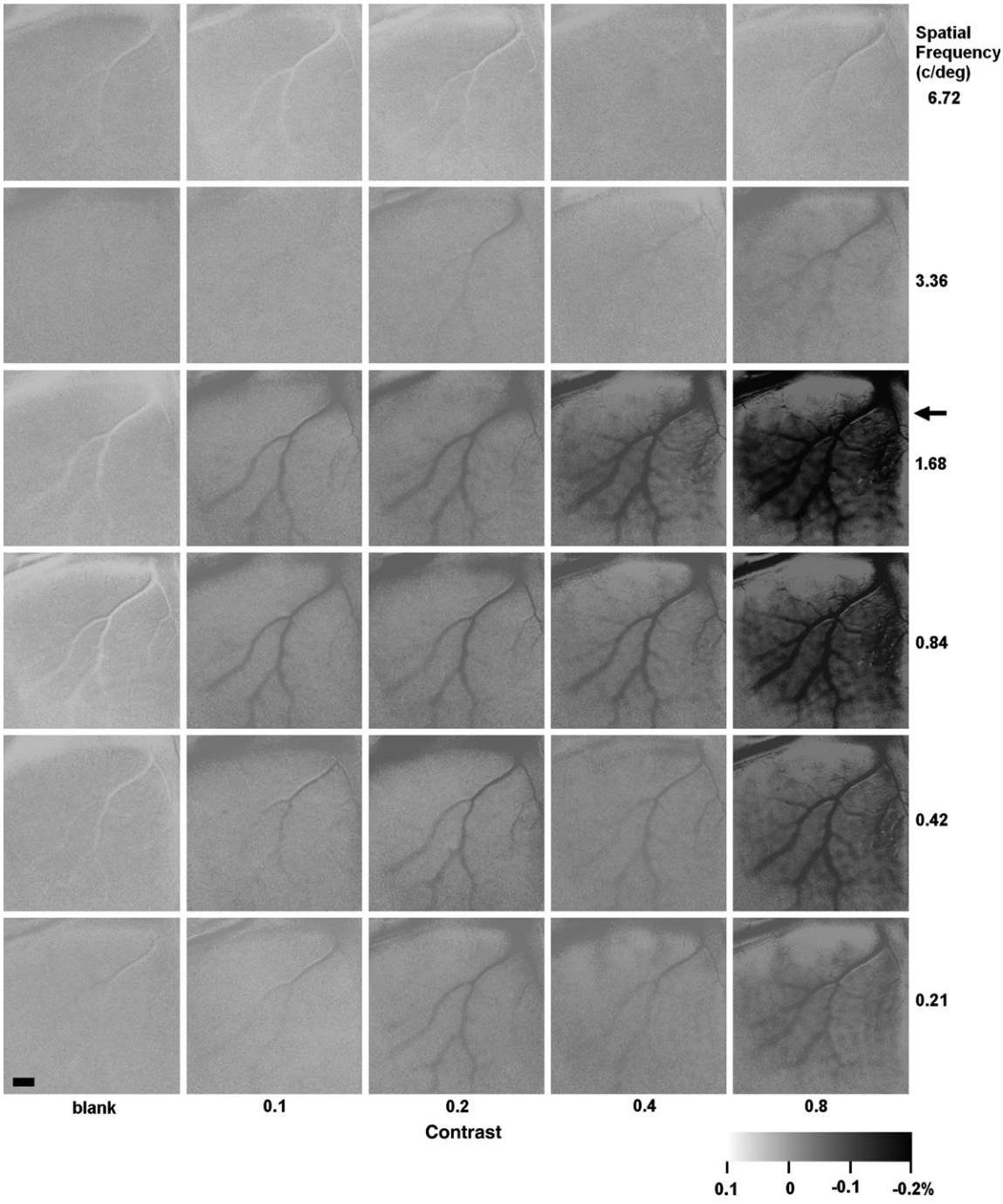

Figure 4. Single-condition maps of V1 and V2 activation to grating stimuli. Thirty single-condition maps in response to horizontal gratings presented at different contrasts (left to right 0, 0.1, 0.2, 0.4, and 0.8 contrasts) and spatial frequencies (bottom to top, 0.21, 0.42, 0.84, 1.68, 3.36, and 6.72 c/deg). Gray level for the maps (dark to bright) represents percent reflectance changes (d*R*/*R*, range: −0.2% to +0.1%, all maps were clipped at the same scale). In general, reflectance increases with contrast. Spatial frequency response is best at 1.68 c/deg and is poorest at 3.36 and 6.72 c/deg. Arrow at right indicates position of V1/V2 border as determined by OD map; applied to all images shown. Scale bar: 1 mm.

for imaging (V2 is almost completely buried in lunate sulcus). Figure 6*A–D* illustrates the blood vessel map (*A*), OD map (*B*, left eye – right eye), orientation map (*C*, horizontal – vertical), and color map (*D*, RG – luminance). These maps were obtained using the same procedures as described in Figure 1. Figure 6*E* illustrates the overlays of orientation domain outlines (blue: horizontal domains, green: vertical domains) and color domains (red dots). In this case, 4 spatial frequencies (0.84, 1.68, 3.36, and 6.72 c/deg) were tested (shown in Fig. 6*F* are responses to horizontal gratings). Similar to the previous case, we observe that V1 response increases with contrast (from 0 to 0.1 to 0.2 to 0.4 to 0.8) and is also modulated by the spatial frequency.

Contrast Response in V1: Color Domains versus Orientation Domains

We examined CRFs of different functional domains in V1. The functional domains were first determined by using the

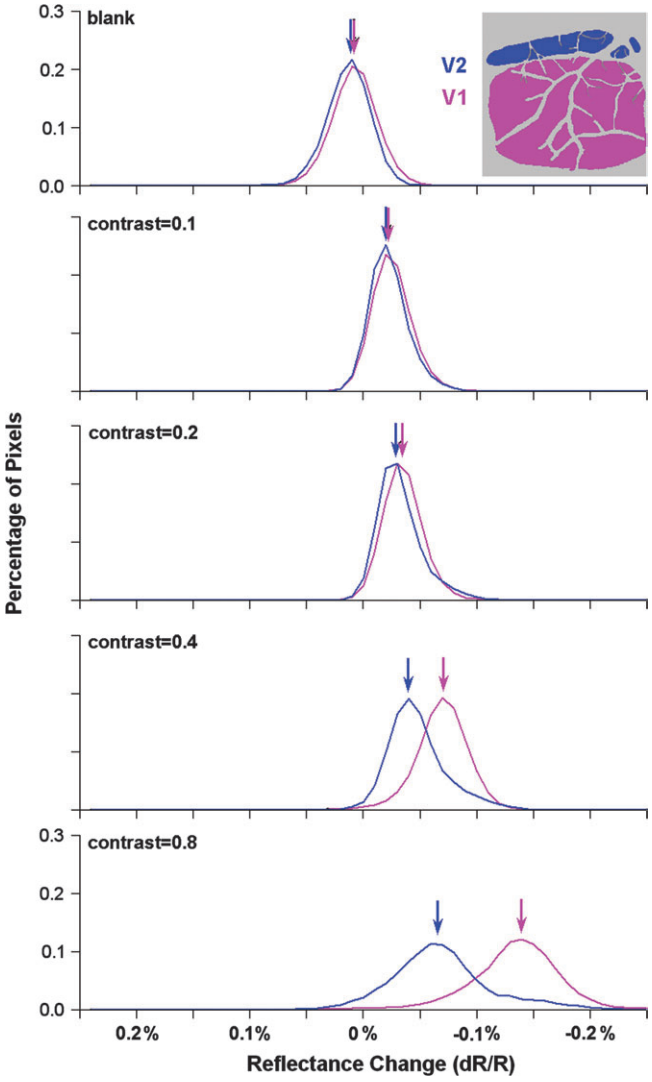

Figure 5. Comparison of V1 and V2 pixel distributions at different stimulus contrasts. Distributions from images obtained in response to stimulus gratings of 1.68 c/deg (average of horizontal and vertical grating responses). Pixel values were taken from entire V1 or V2 region (major blood vessels excluded, see inset at the top). Pink line: V1 pixel distribution; blue line: V2 pixel distribution. Total of 119 364 pixels from V1 and 21 633 pixels from V2 (blue) were used to calculate the distributions. Each distribution contains 50 bins. Arrows above indicate means. Reflectance change from baseline is plotted on *x* axis. Percentage of pixels plotted on *y* axis (scale on top and bottom graphs apply for all). Reflectance change increases with contrast for both V1 and V2; however, imaged response in V1 is relatively stronger for most of the contrast levels.

thresholding method (see Fig. 2). The same functional domain masks were then applied to different contrast response maps to obtain contrast response. Figure 7 illustrates contrast sensitivity functions calculated from the 2 cases illustrated in Figures 4 and 6.

Linear Response Functions for Color Domains and Orientation Domains in V1

Figure 7*A* illustrates the domain masks obtained from functional maps of the second case (Fig. 6). Blue and green outlines indicate locations of horizontal and vertical domains, respectively. Red dots indicate locations of color domains. CRFs from color domains and orientation domains are shown in Figure 7*B,C* obtained at 4 spatial frequencies are shown (0.84 c/deg, purple; 1.68 c/deg, red; 3.36 c/deg, black; 6.72 c/deg, blue). Because horizontal and vertical domains exhibited indistinguishable curves, their averaged values are plotted in Figure 7*C*.

Both linear fitting and hyperbolic curve fitting $[R{=}R_{\max}\times C^n/(C^n+C_{50}^n)]$ (Albrecht and Hamilton 1982) were tested. Results show that, for V1, linear fitting is better than hyperbolic (mean R^2: linear 0.98 ± 0.02, hyperbolic 0.95 ± 0.02, paired *t*-test, $P < 0.005$). Moreover, for each contrast and spatial frequencies, similar reflectance values were obtained for these 2 domain types (compare Fig. 7*B,C*). For example, at the highest contrast (0.8) and optimal spatial frequency (1.68 c/deg, red) similar maximum reflectance values were obtained for color domains (–0.125 ± 0.026%, Fig. 7*B* red line) and orientation domains (–0.14 ± 0.029%, Fig. 7*C* red line). Contrast gain for 1.68 c/deg gratings (red) at 0.8 contrast is –15.6% (per percent contrast change) for color domains (Fig. 7*B* red line) and –17.4% for V1 orientation domains (Fig. 7*C* red line). These values do not differ significantly for color domains and orientation domains.

Figure 7*D–I* illustrates results of contrast imaging from the first case. In this case, the imaged area contains both V1 and V2. Figure 7*D* illustrates the V1 domains: color domain (red outlines), horizontal (blue), and vertical (green) orientation domain masks. In this case, we presented 6 spatial frequencies. Figure 7*E,F* plots V1 CRFs for each of these spatial frequencies (0.21 c/deg, green; 0.42 c/deg, blue; 0.84 c/deg, purple; 1.68 c/deg, red; 3.36 c/deg, black) (the highest spatial frequency, 6.67 c/deg, produced virtually flat curves and so is not plotted). Similar to the previous case, both color domains and orientation domains in V1 exhibit linear contrast response. Maximal values occur at 1.68 c/deg for both color domains (–0.15 ± 0.026%, Fig. 7*E* red line) and orientation domains (–0.14 ± 0.031%, Fig. 7*F* red line); these values do not differ significantly for color domains and orientation domains.

Because electrophysiological findings suggest that blob centers (<100 μm diameter) contain a proportion of high-contrast sensitivity neurons consistent with magno-dominated input (Edwards et al. 1995), we also specifically examined the effect of selecting different size domains. We selected circular areas (60, 120, 180, 240, 300 μm in diameter) centered at maximum response point in individual domains. We found the response varies little when domain size changes. For example, at 0.8 contrast, the average color domain response only changed 1% (see Fig. 8, from 0.00144 to 0.00143) as diameter increases from 60 to 320 μm. Similarly, response at 0.1 contrast was unchanged for different area domain sizes (Fig. 8). Paired *t*-tests revealed no significant difference for these different diameters (all $P > 0.05$). Thus, these linear contrast response curves are robust across multiple domain selection methods and indicate a homogeneity of contrast response within V1.

V2: Thin, Pale, and Thick Domains

Comparison with V1 Domains

Contrast–response curves for V2 color (thin stripes) and V2 orientation (thick/pale stripes) domains are plotted in Figure 7*H,I*. Corresponding domains were illustrated in Figure 7*G* (red: thin stripes, blue: horizontal orientation domains, green: vertical orientation domains). V2 domains show a nonlinearity in the CRFs. Whereas for V1 data, linear fitting is better than hyperbolic, for V2 a hyperbolic function yields better fits (mean R^2: linear 0.85 ± 0.11, hyperbolic 0.93 ± 0.03, paired *t*-test between linear and hyperbolic,

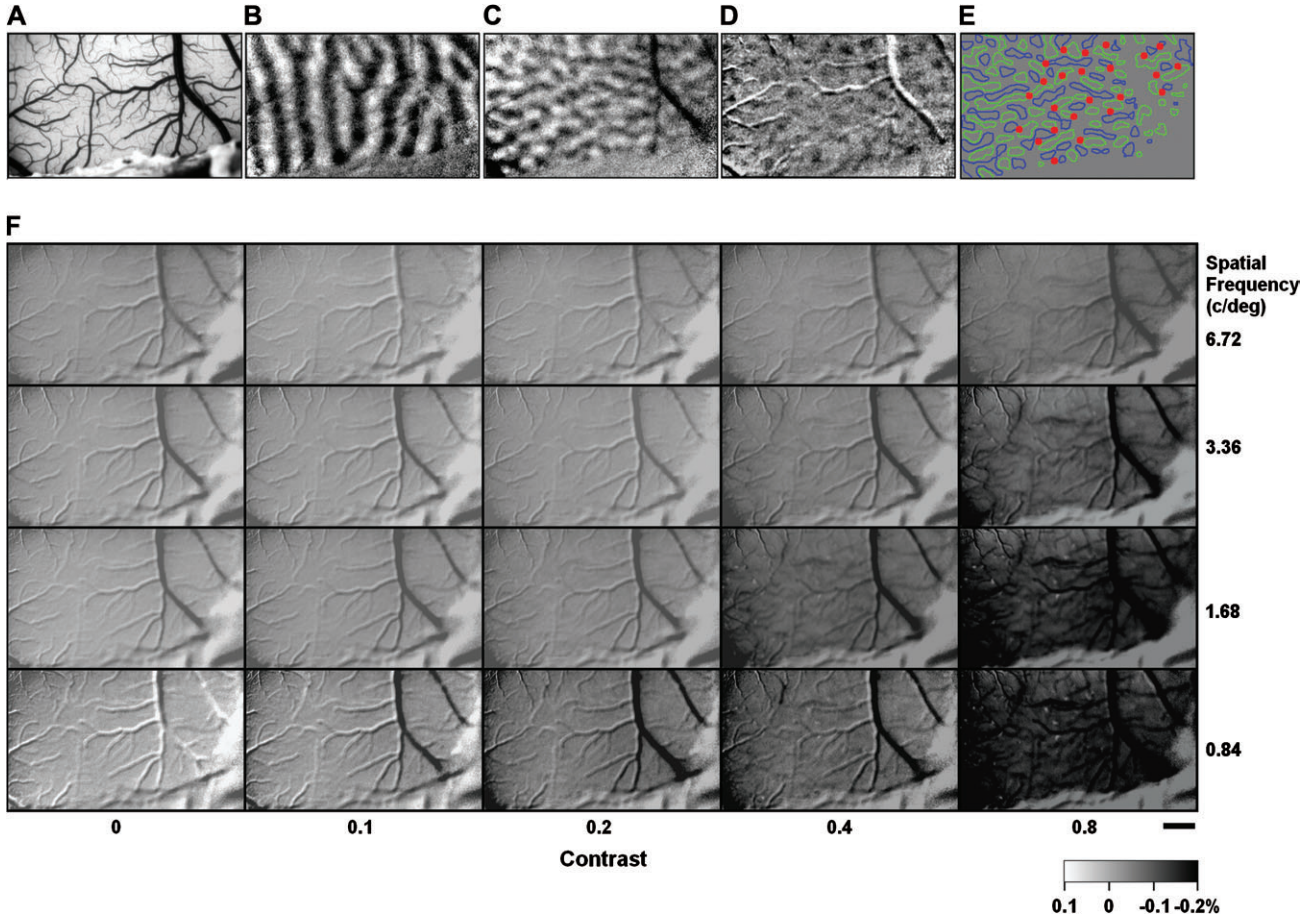

Figure 6. Contrast response in V1 (a second case). (*A*) Blood vessel map, lunate sulcus is on the top (out of field of view). (*B*) OD map (left eye minus right eye). (*C*) Orientation map (horizontal minus vertical). (*D*) Color map (RG minus luminance), (*E*) functional domain outlines: horizontal domain (blue), vertical domain (green), and color domains (red). Because of the high noise level in color map, color domains were manually selected (see Methods). Horizontal and vertical domains were obtained via thresholding method. (*F*) Single-condition maps of optical response to horizontal gratings at different spatial frequencies (0.84, 1.68, 3.36, and 6.72 c/deg) and contrast (0, 0.1, 0.2, 0.4, and 0.8). Gray level for the maps (dark to bright) represents percent reflectance changes (d*R*/*R*, range: −0.2% to +0.1%, all maps clipped at the same scale). Optical response increases with contrast and is best at 0.84–0.68 c/deg and is poorest at 6.72 c/deg. Sum of 25 Trials. Scale bar: 1 mm.

$P < 0.05$). At low contrasts, V1 and V2 have comparable response magnitudes. For example, at 0.1 contrast level, in response to 1.68 c/deg gratings (red lines), the average responses are 0.025% for V1 color domains, 0.024% for V1 orientation domains, 0.028% for V2 thin stripes, and 0.024% for V2 thick/pale stripes. However, whereas V1 responses continue to increase with increasing contrast, V2 CRFs begin to flatten out around contrast levels of 0.2–0.4 and saturate in the mid- to high-contrast range (>0.4).

Color-Activated Domains and Contrast

To examine the possibility of high contrast response within color domains, we examined subtractions of high minus low contrast. However, subtractions at each of 6 spatial frequencies (0.21, 0.42, 0.84, 1.68, 3.36, and 6.72 c/deg) failed to reveal any patterned activation reminiscent of domain activation (not shown). Although electrophysiological studies show that contrasts lower than 10% can elicit magnocellular-specific response, our experience is that at contrasts below 10% the optical signal is quite weak and little activation is elicited.

Comparison of Thin, Thick, and Pale Stripes

We also examined the CRFs for V2 pale stripes and V2 thick stripes but found contrast response of orientation domains across the extent of the thick/pale stripes did not differ. For simplicity of display, we have therefore, combined values for V2 thick and pale stripes (Fig. 7*I*).

Unlike the homogeneity of contrast response in V1, V2 thin and thick/pale stripes exhibit differential contrast response. At the lowest contrasts 0.1–0.2, differences between thin and thick/pale did not reach significance. However, at the highest contrast levels (0.8) and some intermediate (0.4) contrast levels, thin stripes were significantly different from thick/pale stripes (significant data points are indicated by circled data symbols in Fig. 7*H*,*I*). For the highest contrast (0.8), thin stripe responses were significantly greater ($P < 0.01$) across a wide range of spatial frequencies (0.21–1.68 c/deg). For example, at the highest contrast of 0.8, the percent change is 0.096 ± 0.036% for thin stripes and 0.067 ± 0.053% for thick/pale (*t*-test, $P < 0.01$). Thus, at low contrasts, thin, thick, and pale stripes as a whole do not differ in the contrast response; however, as contrast increases thin stripe response tends to increase, whereas thick/pale stripe response tends to saturate.

Figures 9 and 10 provide a spatial view of the different responses between thin and thick/pale stripes in 2 cases. In Figure 9*B* (case 1), the locations of thin, pale, and thick stripes revealed by cytochrome oxidase staining are shown. As shown

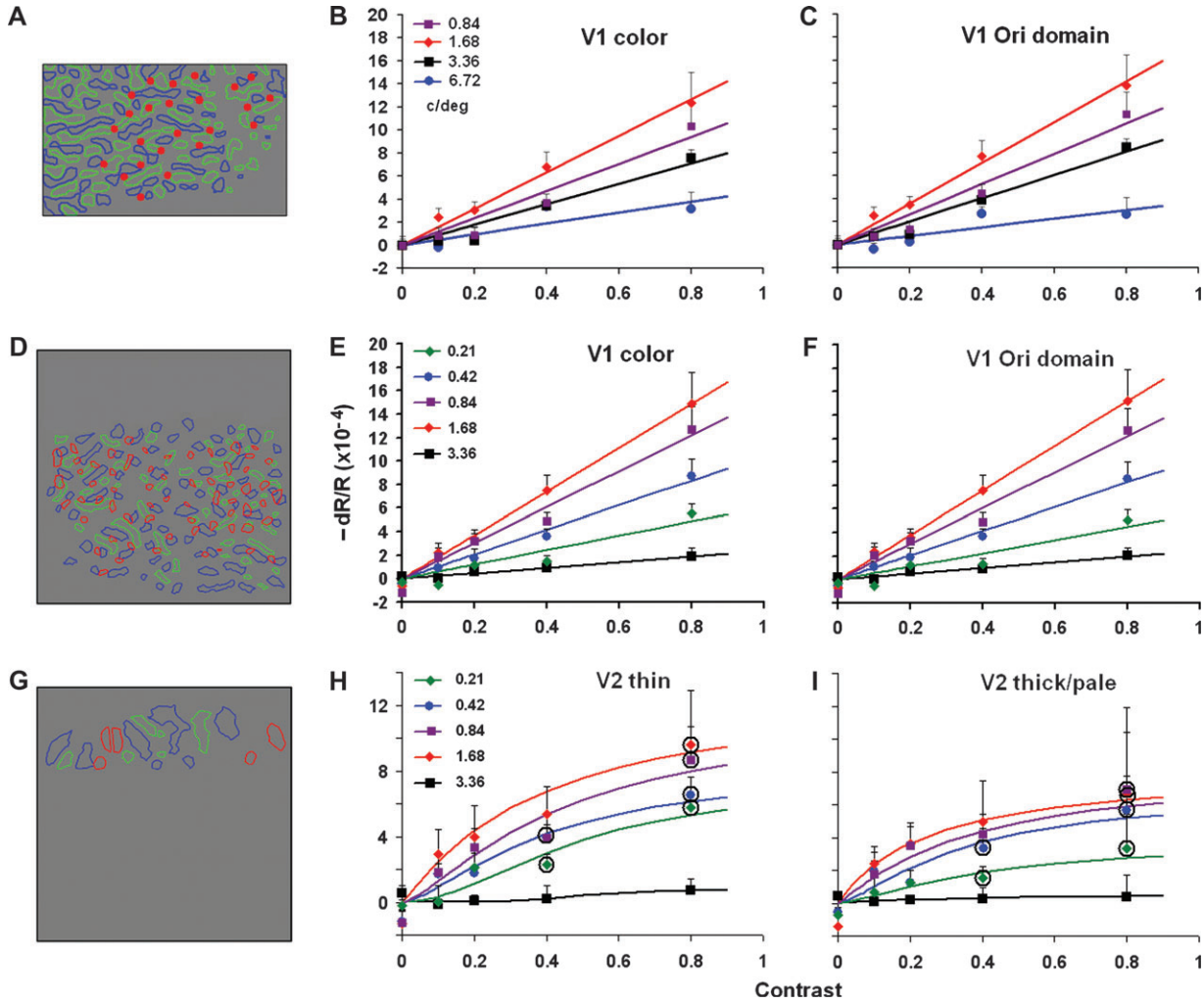

Figure 7. Contrast response of color domains and orientation domains. (*A–C*) V1 from case 2; (*D–F*) V1 from case 1; (*G–I*) V2 from case 1. (*A*) Overlay of 3 V1 functional domain masks in case 2: color domain mask (red dots), horizontal orientation mask (blue outlines), and vertical orientation mask (green outlines), same as Figure 6*E*. (*B*, *C*) CRF of color domains (*B*) and orientation domains (*C*). Four different spatial frequencies are shown (0.84 c/deg, purple; 1.68 c/deg, red; 3.36 c/deg, black; 6.72 c/deg, blue). (*D*) Overlay of 3 functional domain masks in V1 of case 1: color mask (red), horizontal orientation mask (blue), and vertical orientation mask (green). (*E*, *F*) CRFs for color domains and orientation domains in V1 of case 1. (*G*) Overlay of 3 functional domain masks in V2 of case 1. (*H*, *I*) CRF of thin stripes (*H*) and thick/pale stripes (*I*). Five different spatial frequencies are shown (0.21 c/deg, green; 0.42 c/deg, blue; 0.84 c/deg, purple; 1.68 c/deg, red; 3.36 c/deg, black; for clarity 6.72 c/deg is not plotted). For all CRF plots, stimulus grating contrast plotted on *x* axis; imaged reflectance change plotted on *y* axis. Data symbols represent original data, and colored lines are fitted curves. For V1, a linear function yields best fit. For V2, hyperbolic function yields better fit. All fitted curves have $R^2 > 0.9$. Error bar: SD.

in Figure 9*D*, imaging for all conditions revealed activation (darkening) in the thin and thick stripes (all), imaging for color minus luminance revealed structured activation in the thin stripes (color), and imaging for horizontal minus vertical revealed orientation domains in the thick/pale stripes (HV). Small arrows in Figure 9*D* indicate thin stripe locations (also marked with red lines below), large arrowheads indicate thick stripe locations (also marked with white line below). Given the locations of thin, pale, and thick stripes determined by cytochrome oxidase staining and by functional imaging, we then determined the response to different contrasts and spatial frequencies. Figure 9*A* shows that, at low spatial frequency and high contrast, activation in thin stripes was stronger (darker) than in neighboring thick/pale stripes. The CRFs of thin (red line) and thick/pale (white line) are plotted in Figure 9*C* (same data as shown in Fig. 7*H,I*, average of 4 spatial frequency conditions: 0.21, 0.42, 0.84, and 1.68 c/deg). In Figure 9*A*, the images framed in red correspond to those conditions that show statistically significant difference between thin and thick/pale activations (circled data points in Fig. 7*H,I*).

In another case (Fig. 10, case 2), a similar trend was observed. Stripe locations were determined by imaging for OD (*A*), orientation (*B*: horizontal minus vertical, *C*: 45 minus 135 deg orientation), and color minus luminance (*D*). These activations are summarized in (*E*) (blue outlines: horizontal, green outlines: vertical, red outlines: color; thin stripe location demarcated by dotted lines). As can be seen from *F–I*, as contrast increases (*F*: 0.1, *G*: 0.2, *H*: 0.4, *I*: 0.8, spatial frequency 0.5 c/deg), activation within the thin stripe increases. At high contrast, this thin stripe activation is greater than that in the adjacent thick/pale stripes (quantified in *J*).

Contrast Response: Orientation Response Preference

Figure 4 illustrates that V1 has greater reflectance values than V2. However, quite a different relationship is observed with

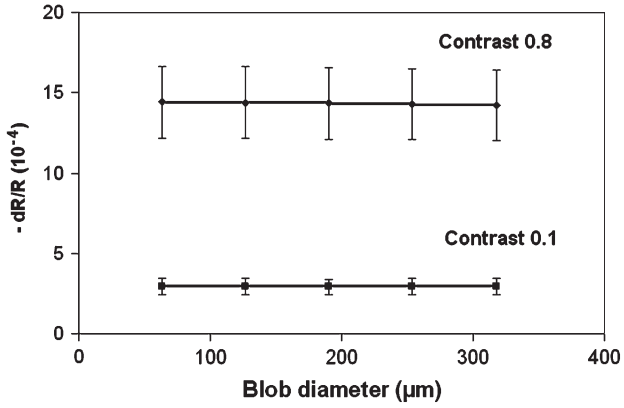

Figure 8. Contrast response with respect to size of domain sampled. At both high (0.8) and low (0.1) contrasts, there is little difference in reflectance value for sample sizes ranging from 60 to 320 μm in diameter. Paired *t*-tests revealed no significant difference for different sample diameters (all $P > 0.05$). This further supports the uniformity of contrast response in V1 across both blob and interblob domains.

respect to response preference magnitudes. Figure 11 illustrates orientation difference maps (horizontal – vertical) for the same case shown in Figure 4. Orientation difference maps (or the "mapping signal") result from subtraction of orthogonal orientations; pixel values in these maps indicate preference for one orientation over another (dark pixels indicate preference for horizontal and light pixels indicate preference for vertical).

In both V1 and V2, we find orientation preference increases with contrast at almost all spatial frequencies. At spatial frequencies of 3.36 c/deg and above, perhaps due to the low response magnitudes, weak orientation preferences are seen. The increase in orientation preference also differs with respect to spatial frequency in V1 and V2: V1 shows greatest differential response at 1.68 c/deg (see Fig. 4, third row of images). V2 also exhibits best response around 1.68 c/deg but displays broader frequency selectivity, exhibiting strong preference even at lower spatial frequencies (strong orientation preferences in V2 are also seen from 0.21 to 1.68 c/deg, see Fig. 11). These features are consistent with the tendencies observed in the raw contrast response shown in Figure 4. From Figures 4 and 5, one might also predict that V2 has weaker orientation preference than V1. However, this is not the case. Figure 11 shows that V2 has at least as strong orientation preference as V1, if not greater.

To examine orientation preference quantitatively, for each map, we examined pixel distributions in V1 and in V2. Each pixel in Figure 11 represents the response difference to 2 orthogonal orientations (0° vs. 90°). We expect a wider pixel distribution for larger difference in cortical response to these 2 orientations (i.e., the greater orientation preference). Pixel distributions in Figure 12*A*,*B* are derived from the orientation domains (both horizontal and vertical) in difference maps in Figure 11. Pixel values were taken from the blood vessel–free V1 or V2 region. For each spatial frequency, different contrast levels are color coded (in reds for V1, Fig. 12*A*; in greens for V2, Fig. 12*B*). Pixel distributions of blank conditions are also provided for comparison (black lines). Surprisingly, at high contrasts (e.g., dark green lines), V2 orientation distribution becomes much wider than V1 curves. This indicates that when contrast increases, V2 domains show larger differential response to orthogonal orientations. This is seen qualitatively in Figure 11, in which the brightest and darkest patches were found in V2.

Figure 12*C* makes the comparison clearer by plotting the SD of the pixel values for different domain types. The bigger the differential response, the greater the SD (the broader the distribution). For each spatial frequency, color domains (dark blue), V1 orientation domains (pink), and V2 thin stripes (red) show slight increase of orientation preference with contrast (relatively flat curves). However, V2 orientation domains (green) show much greater increases at higher spatial frequencies (especially 0.84, 1.68 c/deg). This means that although V2 has overall lower response magnitude than V1, orientation selectivity in V2 is higher than that in V1.

Stability of Orientation Domains with Contrast

In the cat, the locations of orientation domains do not change in position either with contrast (i.e., contrast invariance, see Carandini and Sengpiel 2004; Zhan et al. 2005) or with spatial frequency (cf., Issa et al. 2000). To examine whether this is also the case in monkey cortex, we compared orientation domains obtained at different contrasts (Fig. 13*A*,*B*) and at different spatial frequencies (Fig. 13*C*,*D*). Figure 13 illustrates domains obtained from maps in response to horizontal (Fig. 13*A*) and vertical (Fig. 13*B*) gratings presented at 0.4 (green) and 0.8 (red) contrasts (spatial frequency [SF] 1.68 c/deg). These domains were obtained with the thresholding method. Each type of domain represents highest or lowest 20% pixels in the orientation maps (e.g., Fig. 11). To express the number of pixels common to a pair of maps, we defined percent overlap as the (number of common pixels)/(number of all pixels in one map). The overlapping pixels (coded in blue) comprise 68% of the total pixels in each orientation mask. Figure 13*C*,*D* shows that orientation domains mapped at different spatial frequencies also bear a high degree of overlap. A comparison of maps obtained with 1.68 and 0.84 c/deg gratings revealed overlaps of 72% and 70% for horizontal (Fig. 13*C*) and vertical (Fig. 13*D* domains, respectively. These overlapping percentages are significantly different from random placing of these domains, which yield only 4% overlap (bootstrap test $P < 0.0001$).

To further evaluate the stability of orientation domains across stimulus conditions, we examined the spatial correlation coefficient between the HV difference maps obtained from the optimal stimulus condition and those from suboptimal stimulus conditions (plotted in Fig. 7*E*,*F*). To get a sense of what a poor correlation might be, we calculated correlation coefficients for randomly placed domains (x and y coordinates randomly selected from frame size range): these yielded only 4% overlap. This value is comparable with the percent overlap obtained between 2 orientation domain sets with ~10 deg difference of orientation preference (estimated from the orientation vector map). Thus, for orientation maps with even a very small difference in orientation selectivity (10 deg), the percent overlap falls precipitously. Figure 13*E* shows correlation of all HV maps (of different SF) obtained at the 0.8 contrast level. The correlation coefficient is calculated between the 1.68-c/deg map and other maps on a pixel-to-pixel bases. Almost all stimuli (except 6.72 c/deg which elicited very weak response levels) exhibited strong correlations (64%, 80%, 83%, 100%, and 57% for 0.21, 0.42, 0.84, 1.68, and 3.36 c/deg, respectively). Figure 13*F* shows correlation of all HV maps (of different contrast) obtained at SF of 1.68 c/deg. Again, except for contrasts that produced extremely weak responses (0.1 contrast level), significant correlations were obtained at 0.2, 0.4, and 0.8 contrast levels.

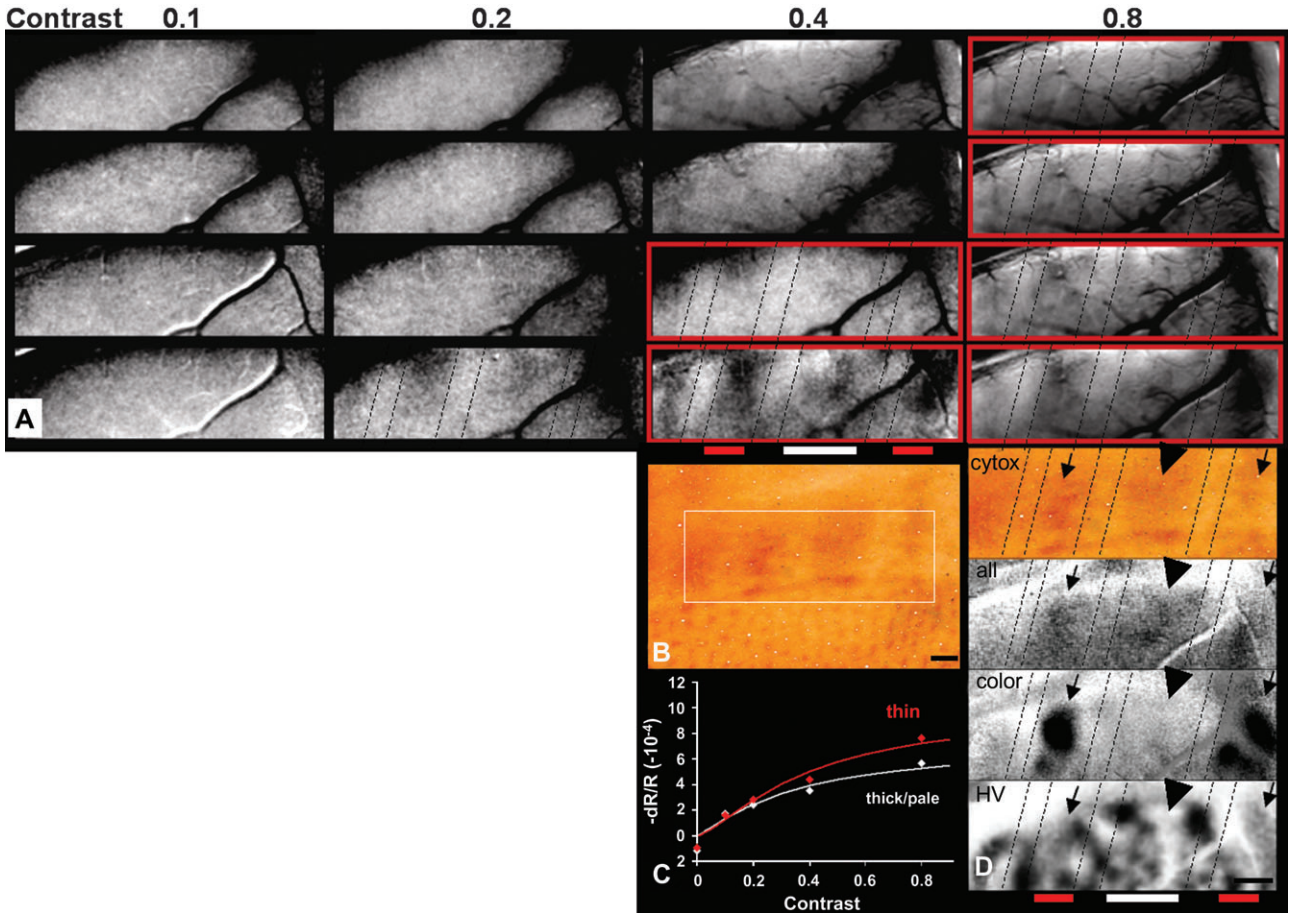

Figure 9. Contrast response in V2 (case 1). (*A*) Responses to 4 spatial frequencies (rows) and 4 contrasts (columns) shown. Each map is average (at each contrast and spatial frequency) of single-condition maps to horizontal and vertical stimuli (no significant difference in maps to these 2 orientations). Conditions framed in red correspond to conditions in Figure 7*H,I* (circled points) that have significant difference between thin and thick/pale stripes. Dotted lines demarcate borders between thin (red bar), pale, and thick (white bar) stripes (see *D*). (*B*) Cytochrome oxidase–stained section through superficial layers of V1/V2. White rectangle indicates region illustrated in (*D*). (*C*) Quantification of reflectance magnitudes in thin (red line) and thick/pale (white line) stripes at different contrasts. (*D*) Approximate locations of thin, pale, and thick stripe borders were determined by cytochrome oxidase–stained tissue (cytox), imaging for general activity (all), color minus luminance (color), and orientation (HV). Small and big arrows indicate thin and thick stripe locations, respectively (also indicated by red and white bars at bottom). Scale bars in (*B*, *D*): 1 mm.

Thus, consistent with previous findings, orientation domains are stable across a range of contrasts and spatial frequencies.

Spatial Frequency Response

Differences in contrast response are further illustrated by examining spatial frequency tuning curves of responses in each of these functional domains. Figure 14*A–D* illustrates, for each of the 4 functional domain types (V1 color domains: blue, V1 orientation domains: pink, V2 thin stripes: red, V2 thick/pale stripes: green), responses plotted with respect to spatial frequency (0.21, 0.42, 0.84, 1.68, and 3.36 c/deg). At low-contrast levels (Fig. 14*A*: 0.1, Fig. 14*B*: 0.2), response is low and there is little difference among different functional domains although some preference for spatial frequency is already apparent. At a contrast level of 0.4 (Fig. 14*C*), differences begin to emerge. A peak response for the near optimal spatial frequency of 1.68 c/deg emerges for both V1 color domains (blue line, obscured by pink line) and V1 orientation domains (pink). This peak spatial frequency response is even more apparent at contrast level 0.8 (Fig. 14*D*). Both color domain and orientation domains peak at 1.68 c/deg and drop steeply on both ends (band pass). Thus, at nearly all spatial frequencies, V1 color domains (blue) and V1 orientation domain (pink) response curves are overlapping.

In V2 (thin stripe: red, thick/pale stripe: green), unlike V1, domains have broader bandwidth and exhibit flatter spatial frequency response at low spatial frequencies end (low pass). Furthermore, unlike the uniformity of response in V1, in V2, thin stripe responses (red) are greater than thick/pale stripe (green) responses at high contrast. In sum, color and orientation domains in V1 show little difference in response with respect to either contrast or spatial frequency. In V2, thin stripes exhibit greater response than thick/pale stripes, especially at high contrast.

The experiments described above were conducted with fixed speeds (4.5 deg/s), so the temporal frequency increases with spatial frequency. Therefore, it is possible the spatial tuning shown in Figure 14*A–D* also reflects the effects of changing temporal frequency (range 0.95–30 Hz, peak at 7.6 Hz.). At higher spatial frequencies, more cycles per second are presented. Ideally, one would like to plot a 2D contrast response surface over both SF and temporal frequency (TF) dimensions. However, practically it is very difficult to include so many conditions in one experiment, primarily because of time constraints and issues of animal stability. It is also difficult to

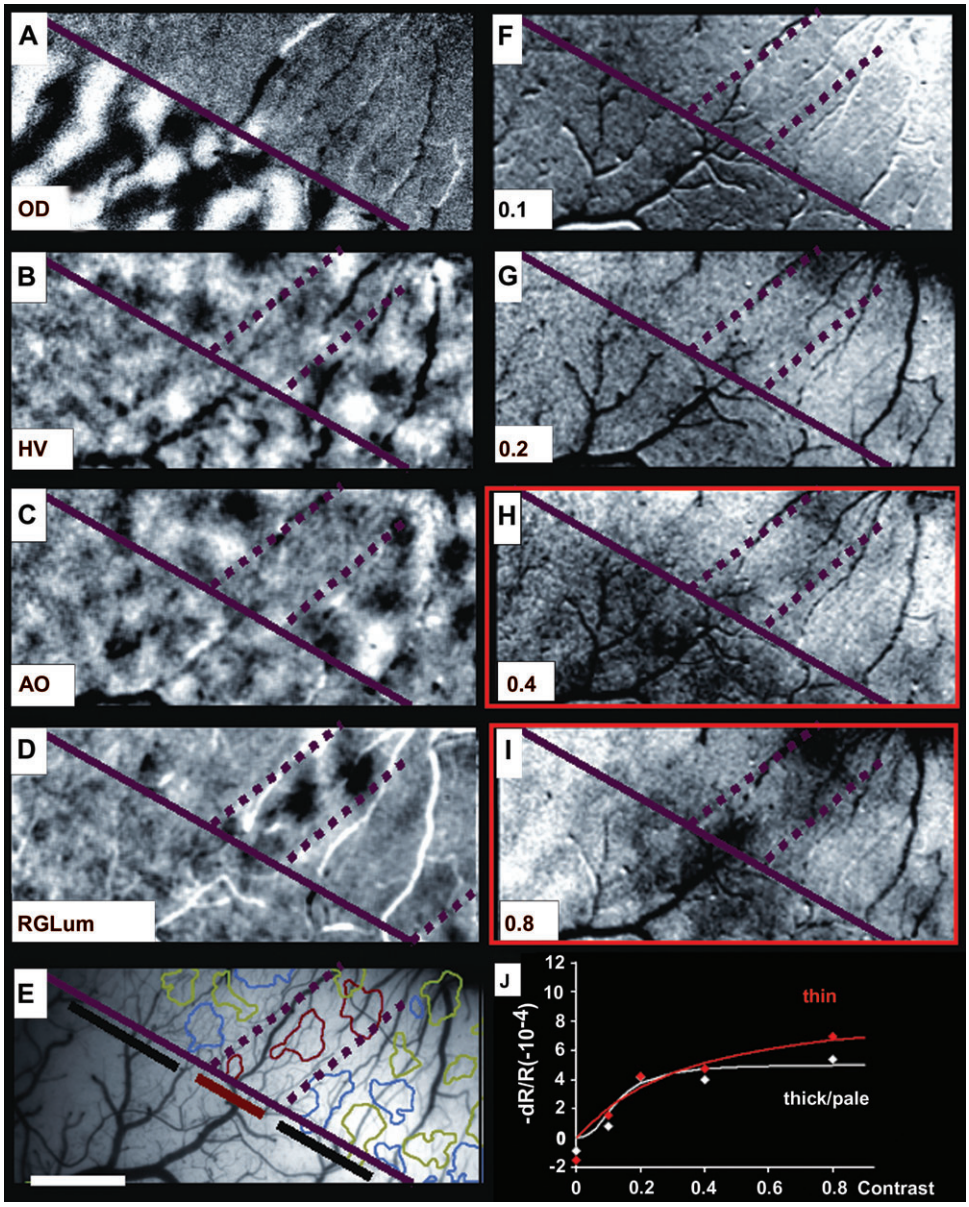

Figure 10. Contrast response in V2 (case 2). (*A–E*) Determination of stripe locations. (*A*) OD map. (*B*) Horizontal minus vertical orientation map. (*C*) 45 minus 135 orientation map. (*D*) Color minus luminance map. (*E*) Summary of color (red outlines), horizontal (blue outlines), and vertical (green outlines) domains. V1/V2 border indicated by solid line, and thin stripe borders indicated by dotted lines. Locations of thin and thick/pale stripes indicated by red and black bars, respectively. (*F–I*) Images obtained in response 0.1, 0.2, 0.4, and 0.8 luminance contrast, respectively. (*J*) CRF of thin (red line) and thick/pale (white line) stripes, respectively. At high contrasts, thin stripes have significantly greater response than thick/pale stripes. Scale bar in (*E*) applies to (*A–I*): 1 mm.

select one "optimal" SF or TF for both V1 and V2. In an attempt to address this issue, in one case, we fixed temporal frequency at 2 Hz and measured spatial tuning (speed range 1–36 c/s). Therefore, lower spatial frequencies were presented at faster speeds and higher spatial frequencies at lower speeds. In this case, we determined the V1/V2 border by imaging OD but did not collect maps of V1 color domains and orientation domains. Pixel values were sampled from all non-blood vessel areas in V1 and in V2. The results are plotted in Figure 14*E*. Comparison of V1 and V2 responses when temporal frequency was fixed reveals 3 points: 1) V1 contrast responses (pink) are still greater than V2 responses (green) overall, 2) V1 responses still peak at 1.68 c/deg, and 3) V2 response peak shifts to slightly lower spatial frequencies (0.84 c/deg). Thus, these data reinforce the findings from the fixed speed experiments and further demonstrate that, at certain temporal frequencies, peak spatial frequency preference in V2 is lower than that in V1.

Spatial Frequency Preference within V2

Electrophysiological studies have revealed some degree of differential spatial frequency preference between stripes in V2 (Levitt et al. 1994; Gegenfurtner et al. 1996; Kiper et al. 1997). To examine whether optical imaging would reveal such spatial frequency preference, we examined single-condition maps at each of 6 spatial frequencies. As shown in Figure 15*A–F*, each map is a general activation map obtained by summing all conditions presented at 1 of 6 spatial frequencies (*A*: 0.21 c/deg, *B*: 0.42 c/deg, *C*: 0.84 c/deg, *D*: 1.68 c/deg, *E*: 3.36 c/deg, and *F*: 6.72 c/deg). Of these 6 spatial frequencies, only the lowest

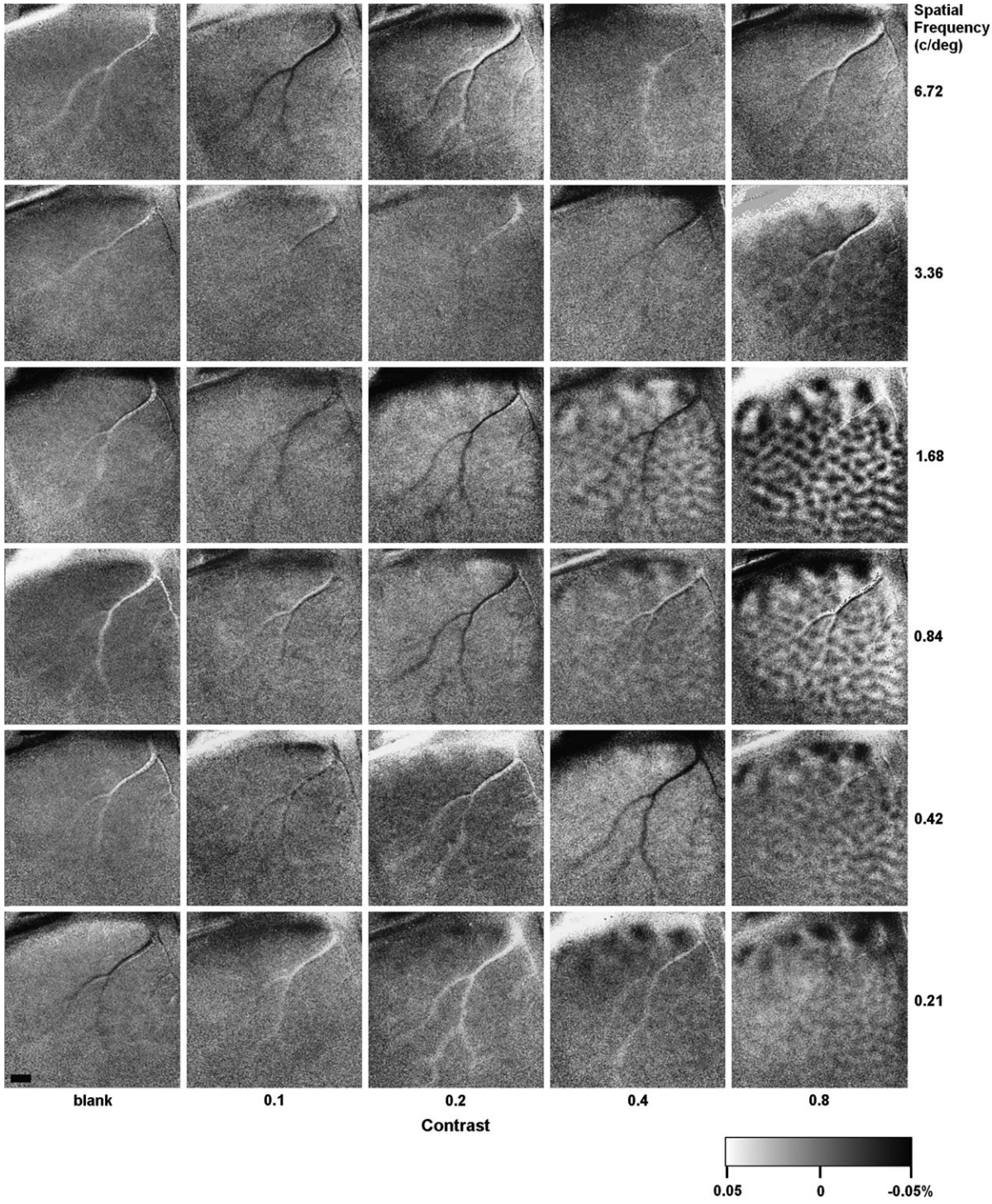

Figure 11. Differential maps (horizontal gratings − vertical gratings) for different spatial frequencies (from bottom to top: 0.21, 0.42, 0.84, 1.68, 3.36, and 6.72 c/deg) and contrasts (from left to right: 0.1, 0.2, 0.4, and 0.8). Same case (case 1) as shown in Figure 4. All maps are displayed using the same gray range (−0.05% to 0.05%) above or below the median for each individual map. In general, response preference increases with contrast. Response preferences at 3.36 c/deg and above are poor. V1 shows greatest differential response at 1.68 c/deg. V2 also exhibits best response around 1.68 c/deg but displays broader frequency selectivity (0.21–1.68 c/deg). Scale bar: 1 mm.

(0.21 c/deg) reveals any structure, one that reveals stronger activations in the thin (thin arrows) and thick (arrowheads) stripes and weaker activations in the pale. Thus, when viewed as a population response across contrasts, preferential low spatial frequency preference is seen in thin and thick stripes in V2. Figure 15*J* plots the measurement of the contrast of pixel gray levels [(thin + thick) – (pale)/(thin + thick) + (pale)] in (*A*–*F*). Only at the lowest spatial frequency do thin and thick stripes have significantly higher response than pale stripes ($P = 0.0067$).

To further compare spatial frequency preference in V2, we examined low minus high spatial frequency maps. This subtraction reveals a pattern that is related to stripe structure in V2 (Fig. 15*G*,*H*). This structured pattern disappears with a middle (1.68 c/deg) minus high (3.36 and 6.7 c/deg) spatial frequency

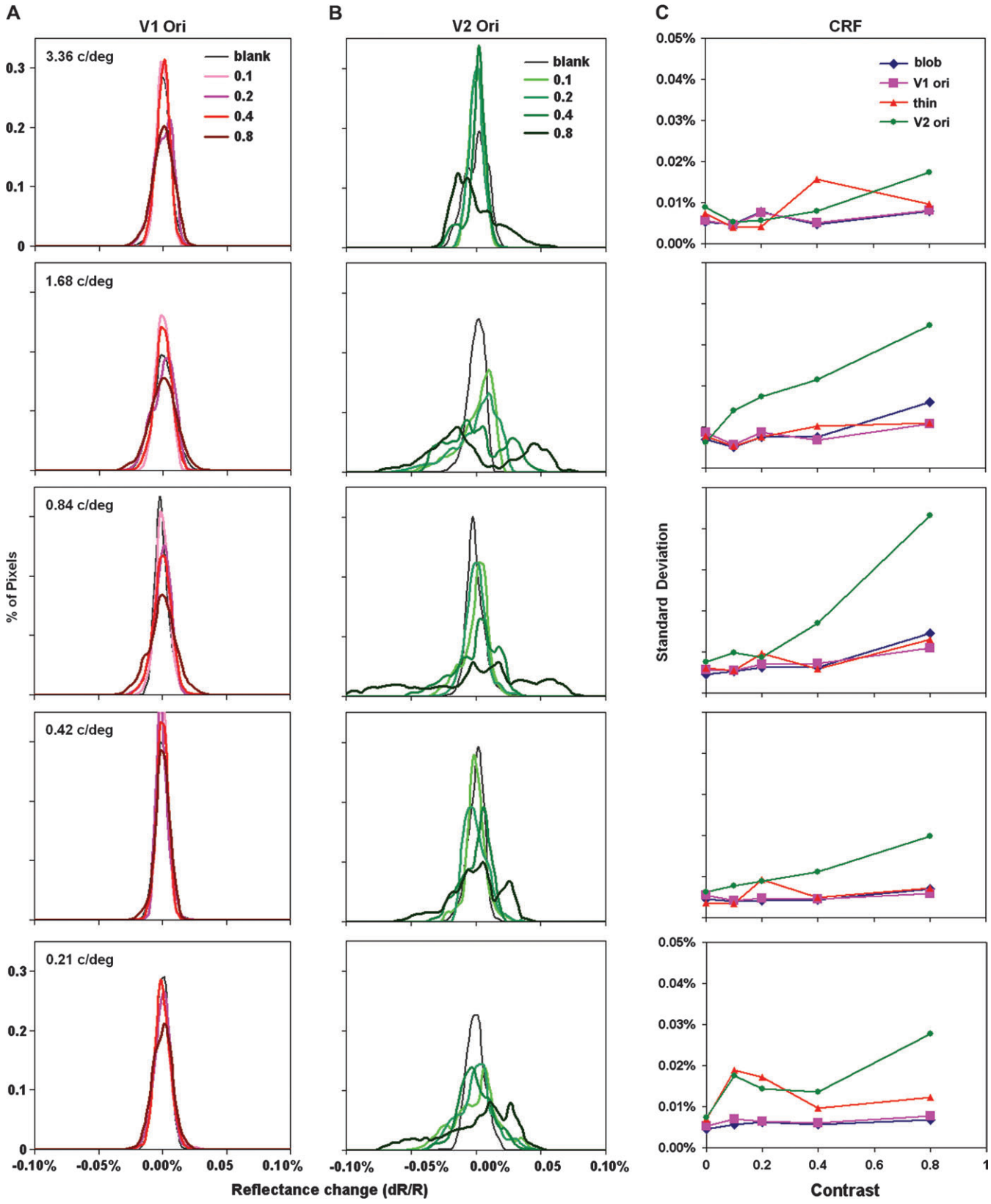

Figure 12. Quantification measurement of orientation selectivity. (*A*, *B*) Pixel value histogram of V1 orientation domains (*A*) and V2 orientation domains (*B*) in response to 5 spatial frequencies. Pixel values were derived from blood vessel–free regions in HV difference maps. Increased orientation preference results in wider and shorter distribution curves. As seen with high-contrast curves (dark green), much greater change is observed in V2 orientation domains than that in V1. Other domain types (V1 color domain, V2 thin stripes) show trends similar to that of V1 orientation domains (not shown). (*C*) SDs of pixel values from different domains (V1 color domains: blue, V1 orientation: pink, thin stripes: red, V2 orientation: green). V2 orientation domains show much higher orientation selectivity at high contrast than all other 3 types of domains.

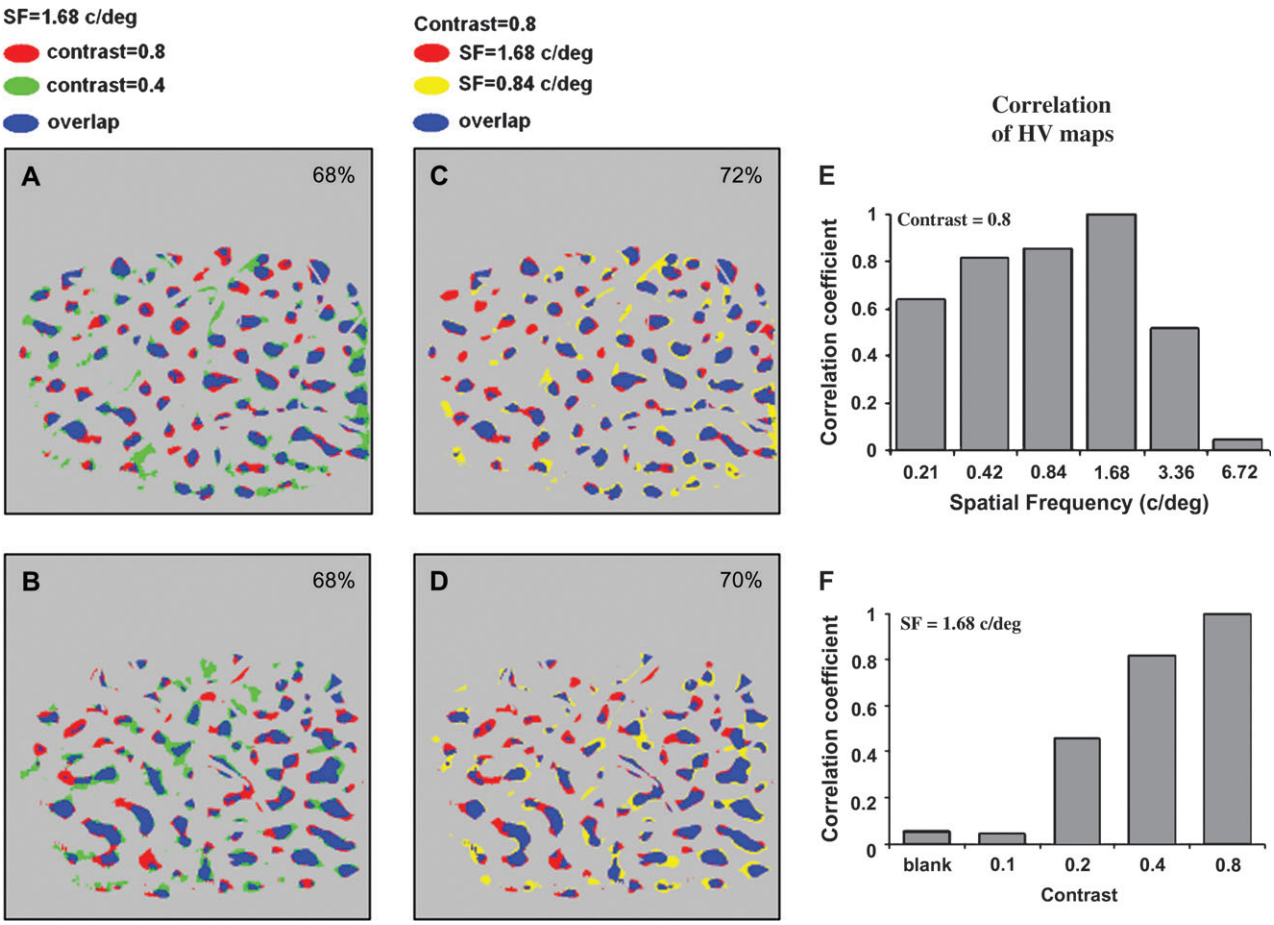

Figure 13. Stability of V1 orientation domains across contrasts and spatial frequencies. (*A–D*) Orientation masks (top 20% of pixel distribution, blood vessels were excluded before thresholding) of horizontal (*A*, *C*) and vertical (*B*, *D*) domains. In all panels, blue indicates overlapping pixels. (*A*, *B*) Comparison of contrast 0.8 (red) and 0.4 (green) maps (both obtained at optimal spatial frequency of 1.68 c/deg) reveals 68% overlap (blue) in both horizontal and vertical domains. (*C*, *D*) Comparison of 1.68 c/deg (red) and 0.84 c/deg (yellow) spatial frequency maps reveals 72% overlap (blue) in horizontal domains and 70% overlap in vertical domains. (*E*, *F*) Spatial correlation coefficients of V1 HV maps. (*E*) correlation values of HV maps obtained at each of 6 different spatial frequencies with that obtained at 1.68 c/deg (contrast 0.8). (*F*) Correlation values of HV maps obtained at each of 5 different contrasts with that obtained at 0.8 (spatial frequency condition 1.68 c/deg).

subtraction (Fig. 15*I*), suggesting that it is not a result of general, nonspecific activity. In Figure 15*H*, color preferring domains (indicated by the white outlines, same case as Fig. 2) are overlaid the images. The arrows indicate thin stripe locations, and the arrowheads indicate thick stripe locations (see Fig. 2). Note that some of the strongest preferences for low spatial frequencies appear to coincide with the thin stripes (regions containing white outlines in V2), consistent with previous electrophysiological reports.

Discussion

Summary

In this study, we measured intrinsic signals from V1 and V2 of the Macaque monkey in response to gratings of different contrasts and spatial frequencies. We found V1 and V2 exhibited different contrast responses. In V1, both color domains and orientation domains exhibit linear contrast response. Unlike V1, V2 domains (thin stripes and thick/pale stripes) exhibit nonlinear contrast response, characterized by high-contrast gain at low contrasts, which saturated at medium-to-high contrasts. In V1, contrast response did not differ between color domains and orientation domains. In V2, at high-contrast levels, thin stripes exhibited higher contrast response than the thick/pale stripes.

Functional Domain Identification

In this study, color domains were located by subtracting cortical response to isoluminant color and luminance gratings (Landisman and Ts'o 2002a; Roe and Lu 2006). Because both color and luminance gratings share the same spatial frequency, average luminance, and drift rate, the only differences between them are the color component and the luminance contrast component. It is unlikely for luminance contrast to underlie the observed structure because luminance contrast maps (high minus low contrast, not shown) have no structure. The remaining color component, therefore, is the basis for the structure revealed by color minus luminance. Our choice of low spatial (0.15–0.5 c/deg) and low temporal frequencies (0.5 Hz) is also aimed at preferentially activating color-selective cells and serves to maximize the strength of the map. At higher spatial/temporal frequencies, the map strength is suboptimal (Roe AW & Lu HD unpublished observations, see also Tootell et al. 1988a; Landisman and Ts'o 2002a).

For identifying orientation domains, we used the best spatial frequency, which is around 1.68 c/deg (see Fig. 11). Increases

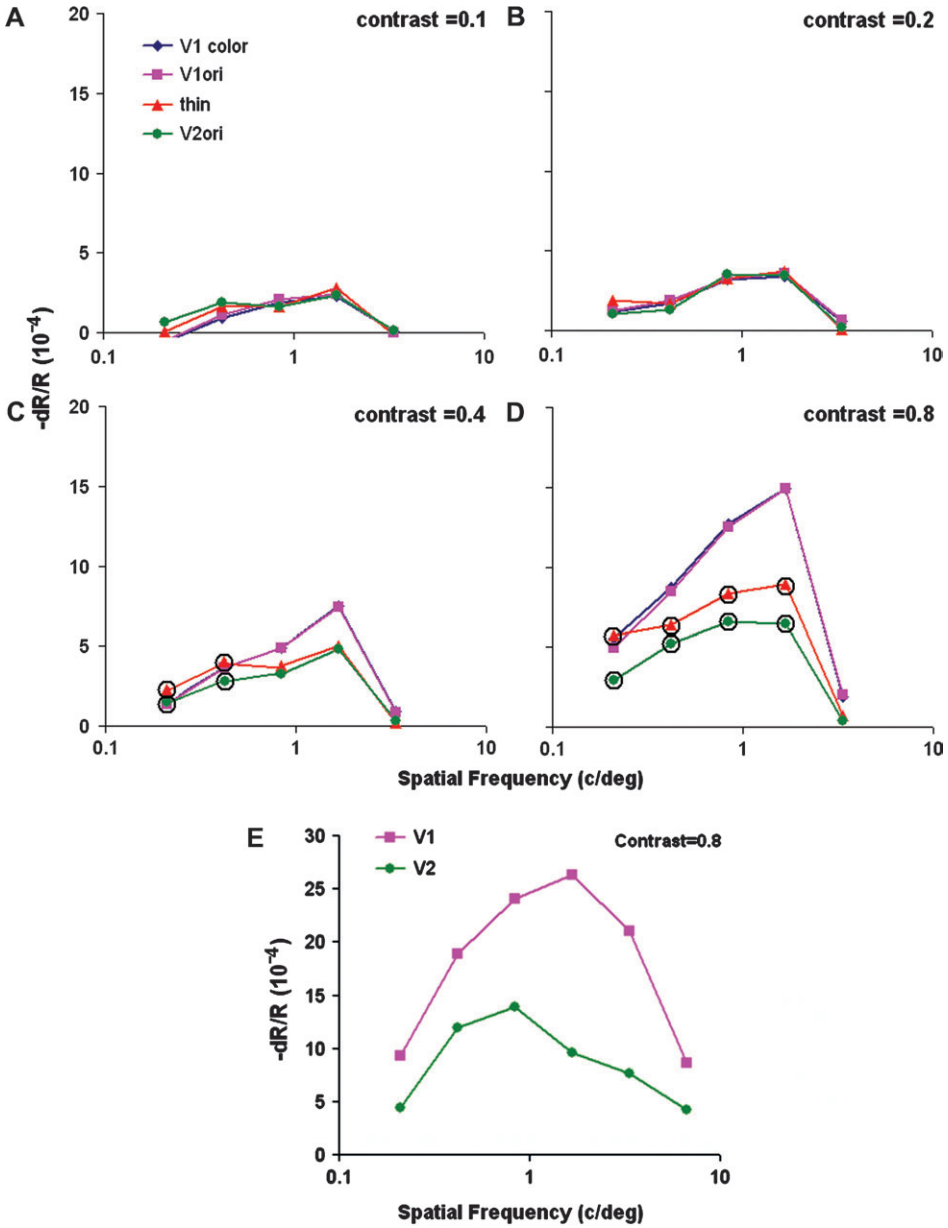

Figure 14. Spatial frequency tuning curves at different contrast levels (*A–D*, fixed speed; *E*, fixed temporal frequency). (*A–D*) From case 1, same data as in Figure 7. At low-contrast levels (contrast = 0.1 and 0.2), all responses are low and spatial tuning is similar. V1 shows stronger response to preferred frequency (1.68 c/deg) than V2 (contrast 0.4 and 0.8). At contrast 0.8, V1 orientation domain (pink) and V1 color domain (dark blue) responses are very similar to each other. V2 (red: thin stripe, green: V2 thick/pale) exhibits lower overall response and broader tuning curves. Compared with V1 curves, V2 curves exhibit more low-pass characteristics (peak between 0.42 and 1.68 c/deg). V2 thin stripes (red) have stronger response than V2 thick/pale stripes (green) at almost all spatial frequencies. (*E*) Spatial tuning curves from case 3 with 0.8 contrast stimuli. Stimuli presented at fixed temporal frequency of 2 Hz. Pixel values were sampled from all non–blood vessel area in V1 and in V2 (based on OD map). In this case, V1 color domains and orientation domains were not available. Similar to experimental data obtained with fixed speeds, 1) V1 responses (pink) are greater than V2 responses (green) overall, 2) V1 responses peak at 1.68 c/deg, and 3) V2 response peak shifts to slightly lower spatial frequencies (0.84 c/deg).

or decreases in spatial frequency reduce the strength of the orientation map. The locations of orientation domains were unchanged across spatial frequencies (see Figs 11 and 13). This observation is consistent with previous findings that orientation selectivity of V1 cells do not depend on spatial frequency of the stimulus (Mazer et al. 2002).

Optical Signal of Contrast Response in Visual Cortex

Optical imaging reveals the summed population response of neurons in a particular cortical region. Although the optical signal is tightly associated with neural activity, it differs from single-unit response in several important ways, ways which may contribute to the differences between CRFs obtained optically and electrophysiologically. The main differences between optical imaging and single-unit recording include the following.

Geometrical Constraints

Because the optical signal arises mainly from the reflectance of superficial layers, neural activity in different layers may not be equally represented in optical imaging maps. In V1, parvocellular signals dominate the superficial layers (layers 2/3 and 4Cβ), whereas magnocellular signals dominate deeper layers (layers

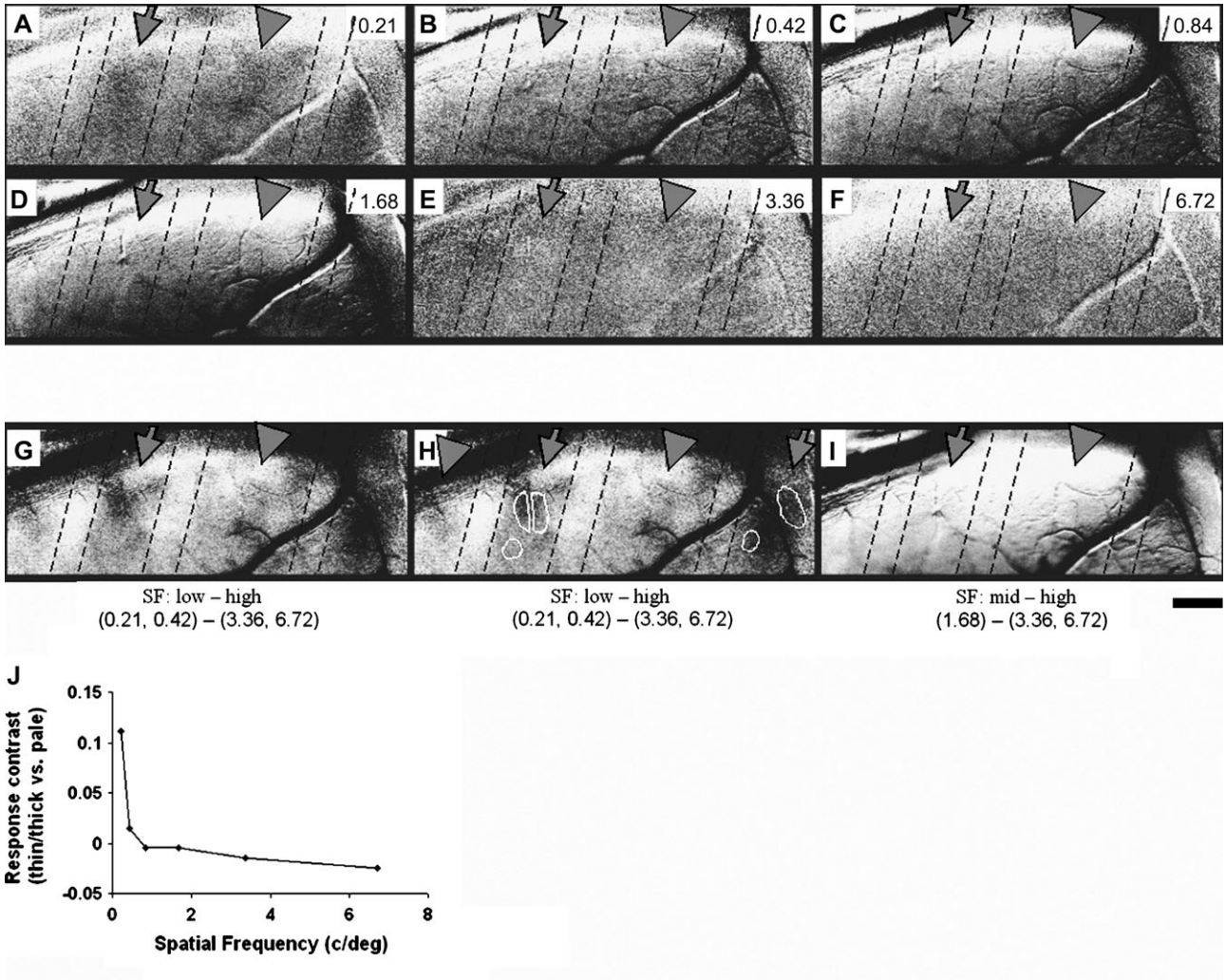

Figure 15. (*A*–*F*) Thin and thick stripes in V2 prefer low spatial frequencies. Each map is sum of all conditions (different contrast and orientation) minus blank obtained at one spatial frequency (spatial frequency listed at top-right corner of the figure in unit of c/deg). Spatial frequencies (*A*: 0.21 c/deg, *B*: 0.42 c/deg, *C*: 0.84 c/deg, *D*: 1.68 c/deg, *E*: 3.36 c/deg, and *F*: 6.72 c/deg). Thin stripes (thin arrows) and thick stripes (arrowheads) have stronger activation in low spatial frequency maps (*A*, and somewhat in *B*) but not high spatial frequency maps (*C*–*F*). (*G*–*I*) Spatial frequency subtraction maps. (*G*) subtraction map: low SF (0.21 and 0.42 c/deg) − high SF (3.36 and 6.72 c/deg) shows structured patterns. (*H*) color domains (white outlines from Fig. 2*B*) overlaid on the low–high SF map shown in (*G*). These alignments suggest that the regions prefer low spatial frequency align with thin stripes (arrows). (*I*) Medium SF (0.84 + 1.68) − high SF (3.36 and 6.72 c/deg) map. The lack of structured patterns in this map further suggests that the pattern in (*A*) is due to low spatial frequency response and not to general activation. All maps in (*G*–*I*) are from subtraction of average horizontal and vertical response obtained at 0.8 contrast. Scale bar: 1 mm. (*J*) Measurement of the contrast of pixel gray levels [(thin + thick) − (pale)/(thin + thick) + (pale)] in (*A*–*F*). Only at the lowest spatial frequency do thin and thick stripes have significantly higher response than pale stripes ($P = 0.0067$).

4Cα, 4B, and 6). Although there is direct koniocellular (blue dominated) input to blobs in the superficial cortical layers, this activity may be weak in response to the luminance contrast gratings we have used. Furthermore, at extrafoveal eccentricities, koniocellular inputs are more similar to parvocellular than magnocellular inputs (Solomon et al. 1999). As a result, parvocellular-like signals may contribute more to the detected contrast responses than magnocellular signals.

Spikes versus Subthreshold Activities

The direct relationship between oximetry and neural activity has not been established. However, several studies provide indirect results that suggest contributions from both action potential and subthreshold membrane activity. For example, according to one estimate based on an energy consumption model of rodent cerebral cortex (Attwell and Laughlin 2001), about 34% of the total energy is consumed by postsynaptic activity compared with 47% for action potentials. Another study by Logothetis et al. (2001), who simultaneously measured local field potential (LFP), single- and multiunit spiking activity, and blood oxygen level–dependent (BOLD) response in monkey visual cortex, suggested that only the LFP linearly correlates with BOLD response. In comparison with spiking activity, BOLD signal showed higher response at low contrast because of the large subthreshold activity. Under some conditions, the subthreshold component may even dominate. For example, in translaminar recordings from V1 and V2 of awake monkeys, there are instances of large amplitude transmembrane currents (due to synaptic activation) with little or no action potential correlates in the superficial cortical layers (cf., Mehta et al. 2000). These and other studies all suggest that hemodynamic response is tightly correlated with the sum of both subthreshold and spiking activity. Therefore, in contrast to spike activity, the optical signal represents not only the outputs of the neurons but

also their input and integrative processes. Finally, any experimental parameters (e.g., anesthesia) that have different effects on spike activity and subthreshold activity will also contribute to observed differences.

Population Response to Single Stimuli

In addition to these differences, stimuli used in optical imaging are not tailored to the preferences of individual neurons. Rather, the measured response is an average response of many neurons, some of which will respond optimally but others suboptimally to a particular stimulus. Thus, the summed contributions from optimally stimulated neurons and suboptimally stimulated neurons are likely to broaden the contrast response at each contrast and, as a result, broaden (and flatten or linearize) the overall population CRF (also see below). The fact that the optical response cannot be fully predicted by single-unit response indicates that the population response is a different measure of cortical activity, one which makes this study necessary.

Linear Response in V1

We find that the CRFs in V1 are fairly linear over the range of contrasts tested (0–0.8, see Fig. 7*A–D*). The linearity revealed by our optical imaging data indicates that V1 response as a population does not saturate as readily as single-unit responses and enables a larger dynamic range. This may be surprising given the known hyperbolic CRFs of V1 neurons (Albrecht and Hamilton 1982). However, as we described above, the optical signal is different from neuronal spiking response in many respects. First, in the imaged responses, each pixel represents the summed activity of hundreds to thousands of neurons and can represent increase in firing rate of single neurons and/or the increase in the number of responsive neurons. As previously shown (Albrecht and Hamilton 1982), summing a population of individual contrast functions in V1 can lead to a relatively linear population CRF. Second, the intrinsic signal reflects both spiking and subthreshold components (e.g., Grinvald et al. 1994; Das and Gilbert 1995). Third, the optical signal represents neural activity of superficial layers where P (and K) signals dominate, consistent with a relatively linear CRF response. Finally, in optical imaging studies, unlike single-unit studies, the visual stimulus is not optimized for single neurons and therefore activates a broad population of neurons. The sum total of such a diverse population would also tend to linearize the response function.

A linear contrast response is also consistent with the view that contrast response in superficial layers of V1 is dominated by P-type response. In fact, in comparison with P neuron input, the number of K or M neuron inputs is relatively small. In the LGN, the P neuron to M neuron ratio is 35:1 in the fovea, 10:1 overall, and 5:1 at an eccentricity of 15 deg (Azzopardi et al. 1999). The number of K neurons is comparable with M neurons (roughly 100 000) and are outnumbered by P neurons by a factor of 10 (Hendry 1994; Hendry and Reid 2000). It also has been shown that P-dominated layer 4Cβ provides 5 times more synapses than 4Cα (M dominated) to layers 2/3 (Yabuta and Callaway 1998), the layers from which optical signals are derived. As a result, it is possible that the reflectance signal derived from M and K neurons may be overwhelmed by those from P neurons. Electrophysiological sampling has indicated that, on average, neurons in layer 2/3 have low-contrast sensitivity, resembling that of parvocellular neurons (Edwards et al. 1995). Because optical imaging reveals the general activity of a certain area, it is very likely the existence of M-driven or K-driven response is not strong enough to be detected from the background P-driven response. In contrast to monkey visual cortex, most visual input to cat visual cortex has high-contrast gain and nonlinear contrast response (Shapley and Victor 1978; Shapley and Perry 1986). Not surprisingly, optical imaging of contrast response in cat reveals nonlinear CRF in both area 17 (Carandini and Sengpiel 2004) and area 18 (Zhan et al. 2005).

Similar Contrast Response for Color Domains and Orientation Domains

V1 blobs receive anatomical inputs from magno-recipient and parvo-recipient layers in V1 as well as direct inputs from koniocellular layers in the LGN; interblobs receive predominantly from parvo-recipient layers (e.g., Lachica et al. 1992; Shostak et al. 2002). The contrast sensitivity of K cells is heterogeneous (Norton et al. 1988). Those recorded in the intermediate K cell layers in bush babies have contrast sensitivity functions that are on average intermediate to those of M and P cells. Consistent with this view, cells recorded in CO blob centers exhibit higher contrast sensitivity than those more distant from blob centers (Edwards et al. 1995). Hubel and Livingstone (1990) also found a tendency for CO blobs to have higher contrast sensitivity than interblobs. However, other studies suggest that this magnocellular input may have a relatively weak influence in the superficial layers. Stimulation with low-contrast (8%) achromatic gratings produces much less activation in layers 2/3 than in layers 4B/4Cα/6, as observed with 2-deoxyglucose (Tootell et al. 1988b; Figs 2, 5, and 7). Other studies fail to find evidence of distinctive M input to the blobs. Nealey and Maunsell (1994) report that inactivation of magnocellular layers in the LGN leads to a similar degree of response reduction in both blobs and interblobs. In cat visual cortex, it has been demonstrated that patches of low spatial frequency response align with cytochrome oxidase blobs (Shoham et al. 1997) and that regions of low spatial frequency response also tend to avoid OD borders (Hubener et al. 1997). Although cats do not have color vision, there appear to be parallels with the primate visual system. It is possible that in cats, the role of blobs is also for processing surface features such as brightness. Similarly, our optical imaging results fail to show preferential activation of color domains or blobs with low-contrast stimuli, even at contrasts below 10%. In fact, the contrast response in V1 is relatively homogeneous. It is likely that the relatively weak magnocellular contribution to the superficial layers is too small to detect with the optical imaging method. It is possible that there is difference in contrast response between blobs and interblobs but that such difference is either too small in amplitude to be detected by the optical signal or that it is obscured by the spatial spread of the optical signal (Das and Gilbert 1995; Malonek and Grinvald 1996). However, the lack of contrast response differences between blob and interblob responses cannot be due solely to the limitations of the methodology, as blobs and interblobs are clearly differentiable with optical imaging of color preference response (Landisman and Ts'o 2002a, b; Roe and Lu 2006). In conclusion, our finding is consistent with previous studies that suggest the degree of magnocellular inputs to the color domains is small and difficult to detect at a population response level.

Greater Response in V2 Thin Stripes

Thin and thick stripes in V2 stain darkly with cytochrome oxidase, indicating that they have a higher basal activity level than pale stripes. Thus, a general activity map obtained by summing all stimulus conditions typically reveals activations (darkening) corresponding to the thin and thick stripes in V2 (Ts'o et al. 1990; Roe and Ts'o 1995). In addition, we often find that thin stripes are easier to be identified (takes fewer trials) in the general map or appear darker than thick stripes. In this study, we find that at low and intermediate contrast levels (0–0.4), thin and thick/pale stripes do not differ much in contrast response. However, at the highest contrast level tested, thin stripes exhibited significantly greater response. Levitt et al. (1994) recorded from different CO compartments in V2 and found that the mean contrast sensitivity (the reciprocal of the threshold contrast) is highest for thick stripes (20.09), intermediate for pale stripes (20.0), and lowest for thin stripes (10.9). However, the other 2 parameters they measured, the mean semisaturation values (thin: 22%; thick: 16%; pale: 14%), and the exponents governing the steepness of the CRFs (thin: 2.46; thick: 2.66; pale: 2.74) are not significantly different among stripes. Our findings at 0–0.4 contrast levels are consistent with their primary conclusion that there was little differentiation between the stripe types with respect to contrast sensitivity.

A major difference between our study and that of some other studies including Levitt's (1994) is that we also tested contrast response at high-contrast levels (0.8). Because many single-unit contrast response curves appear to saturate above 0.4–0.5, higher contrasts are often not tested. We suggest that at higher contrast levels, thin stripe cells, either as single units or as a population, continue to signal contrast change, whereas those in thick and pale stripes tend to saturate. Our data are consistent with a strong blob-derived input to the thin stripes: we suggest that thin stripes may be dominated by P input at high contrasts and by (blob derived) M input at low contrasts. Such M contribution could become enhanced (to levels detectable by our optical imaging methods) via blob convergence onto thin stripes (cf., Roe and Ts'o 1999). In addition, there is direct K input to V2, especially prominent in foveal regions of V2 (Hendry 1994). Evidence suggests that direct thalamic input targets primarily the thick and thin stripes of V2 (Levitt et al. 1995; Hendry and Reid 2000); however, little is known about the functional properties of these extrastriate-projecting neurons. The possibility remains that there is K contribution to the observed thin stripe activation at high contrasts.

Our data are consistent with differential P versus M contribution in V2 stripes at a population response level. Merigan and Maunsell (1993) and Allison et al. (2000) found that M inactivation led to contrast sensitivity loss at all contrasts tested but was most prominent at the lowest contrasts. P inactivation led to contrast sensitivity loss primarily at the highest contrasts tested and made little difference at low contrasts. Our data suggest that the perceptual importance of P input at high-contrast levels (Merigan and Maunsell 1993) is evident at a population level in V2.

Relationship to Brightness Perception

Cortical neurons that respond to diffuse brightness change have been found in visual cortex of both cat and monkey (Kayama et al. 1979; DeYoe and Bartlett 1980; Rossi et al. 1996; Hung et al. 2001; Kinoshita and Komatsu 2001; Peng and Van Essen 2005; Roe et al. 2005). These neurons often have large RFs, and some have weak orientation selectivity. Our recent study shows that there are cells in visual cortex that respond to brightness change (both real luminance change and illusory [edge induced] brightness change) and that these brightness responses are preferentially localized in V2 thin stripes (Roe et al. 2005). Consistent with this finding, our results here show that at higher contrast, thin stripes may continue to signal contrast change, whereas thick and pale stripes become relatively saturated. Indeed, such a large dynamic range would be desirable for a system that encodes brightness information. Together, these results support the view that thin stripes play a strong role in the processing of brightness information and further support the view that thin stripes are preferentially involved in the processing of surface properties such as color and brightness (cf., Hubel and Livingstone 1987; Xiao et al. 2003).

Supplementary Material

Supplementary material can be found at http://www.cercor.oxfordjournals.org/.

Notes

We thank Michael Kraus for assistance on an initial experiment. This work was supported by the National Institutes of Health EY11744, Packard Foundation, Center for Integrative and Cognitive Neuroscience, and P30EY008126. *Conflict of Interest*: None declared.

Funding to pay the Open Access publication charges for this article was provided by NIH EY117440.

Address correspondence to Haidong D. Lu, Department of Psychology, Vanderbilt University, 301 Wilson Hall, 111 21st Avenue South, Nashville, TN 37203, USA. Email: haidong.lu@vanderbilt.edu.

References

Albrecht DG, Hamilton DB. 1982. Striate cortex of monkey and cat: contrast response function. J Neurophysiol. 48(1):217–237.

Allison JD, Melzer P, Ding Y, Bonds AB, Casagrande VA. 2000 Jan–Feb. Differential contributions of magnocellular and parvocellular pathways to the contrast response of neurons in bush baby primary visual cortex (V1). Vis Neurosci. 17(1):71–76.

Attwell D, Laughlin SB. 2001. An energy budget for signaling in the grey matter of the brain. J cereb blood flow metabol. 21:1133–1145.

Azzopardi P, Jones KE, Cowey A. 1999. Uneven mapping of magnocellular and parvocellular projections from the lateral geniculate nucleus to the striate cortex in the macaque monkey. Vision Res. 39(13):2179–2189.

Bartfeld E, Grinvald A. 1992. Relationships between orientation-preference pinwheels, cytochrome oxidase blobs, and ocular-dominance columns in primate striate cortex. Proc Natl Acad Sci USA. 89(24):11905–11909.

Blasdel GG, Lund JS, Fitzpatrick D. 1985. Intrinsic connections of macaque striate cortex: axonal projections of cells outside lamina 4C. J Neurosci. 5(12):3350–3369.

Carandini M, Sengpiel F. 2004. Contrast invariance of functional maps in cat primary visual cortex. J Vis. 4(3):130–143.

Chatterjee S, Callaway EM. 2003. Parallel colour-opponent pathways to primary visual cortex. Nature. 426:668–671.

Chen LM, Friedman RM, Ramsden BM, LaMotte RH, Roe AW. 2001. Fine-scale organization of SI (area 3b) in the squirrel monkey revealed with intrinsic optical imaging. J Neurophysiol. 86(6):3011–3029.

Chen Y, Kaplan E. 2003. The dependence of the intrinsic optical signal amplitude on stimulus contrast. Neuroscience abstract 2003, 69.18.

Contreras D, Palmer L. 2003. Response to contrast of electrophysiologically defined cell classes in primary visual cortex. J Neurosci. 23(17):6936–6945.

Das A, Gilbert CD. 1995. Long-range horizontal connections and their role in cortical reorganization revealed by optical recording of cat primary visual cortex. Nature. 375(6534):780–784.
DeYoe EA, Bartlett JR. 1980. Rarity of luxotonic responses in cortical visual areas of the cat. Exp Brain Res. 39(2):125–132.
Dumoulin SO, Baker CL, Hess RF, Evans AC. 2003. Cortical specialization for processing first- and second-order motion. Cereb Cortex. 13(12):1375–1385.
Edwards DP, Purpura KP, Kaplan E. 1995. Contrast sensitivity and spatial frequency response of primate cortical neurons in and around the cytochrome oxidase blobs. Vision Res. 35(11):1501–1523.
Gegenfurtner KR, Kiper DC, Fenstemaker SB. 1996. Processing of color, form, and motion in macaque area V2. Vis Neurosci. 13(1):161–172.
Grinvald A, Lieke EE, Frostig RD, Hildesheim R. 1994. Cortical point-spread function and long-range lateral interactions revealed by real-time optical imaging of macaque monkey primary visual cortex. J Neurosci. 14(5 Pt 1):2545–2568.
Hendry SHC. 1994. Immunocytochemical and quantitative analyses of a third geniculocortical population in the macaque LGN. Invest Opthalmol Vis Sci. 35:1975.
Hendry SHC, Calkins DJ. 1998. Neuronal chemistry and functional organization in the primate visual system. Trends Neurosci. 21(8):344–349.
Hendry SHC, Reid RC. 2000. The koniocellular pathway in primate vision. Annu Rev Neurosci. 23:127–153.
Hubel DH, Livingstone MS. 1987. Segregation of form, color, and stereopsis in primate area 18. J Neurosci. 7(11):3378–3415.
Hubel DH, Livingstone MS. 1990. Color and contrast sensitivity in the lateral geniculate body and primary visual cortex of the macaque monkey. J Neurosci. 10(7):2223–2237.
Hubener M, Shoham D, Grinvald A, Bonhoeffer T. 1997. Spatial relationships among three columnar systems in cat area 17. J Neurosci. 17(23):9270–9284.
Hung CP, Ramsden BM, Chen LM, Roe AW. 2001. Building surfaces from borders in Areas 17 and 18 of the cat. Vision Res. 41(10-11): 1389–1407.
Issa NP, Trepel C, Stryker MP. 2000. Spatial frequency maps in cat visual cortex. J Neurosci. 20(22):8504–8514.
Kalatsky VA, Polley DB, Merzenich MM, Schreiner CE, Stryker MP. 2005. Fine functional organization of auditory cortex revealed by Fourier optical imaging. Proc Natl Acad Sci USA. 102(37): 13325–13330.
Kaplan E, Shapley RM. 1982. X and Y cells in the lateral geniculate nucleus of macaque monkeys. J Physiol. 330:125–143.
Kayama Y, Riso RR, Bartlett JR, Doty RW. 1979. Luxotonic responses of units in macaque striate cortex. J Neurophysiol. 42(6):1495–1517.
Kinoshita M, Komatsu H. 2001. Neural representation of the luminance and brightness of a uniform surface in the macaque primary visual cortex. J Neurophysiol. 86(5):2559–2570.
Kiper DC, Fenstemaker SB, Gegenfurtner KR. 1997. Chromatic properties of neurons in macaque area V2. Vis Neurosci. 14(6):1061–1072.
Lachica EA, Beck PD, Casagrande VA. 1992. Parallel pathways in macaque monkey striate cortex: anatomically defined columns in layer III. Proc Natl Acad Sci USA. 89(8):3566–3570.
Landisman CE, Ts'o DY. 2002a. Color processing in macaque striate cortex: relationships to ocular dominance, cytochrome oxidase, and orientation. J Neurophysiol. 87(6):3126–3137.
Landisman CE, Ts'o DY. 2002b. Color processing in macaque striate cortex: electrophysiological properties. J Neurophysiol. 87(6):3138–3151.
Lennie P, Krauskopf J, Sclar G. 1990. Chromatic mechanisms in striate cortex of macaque. J Neurosci. 10(2):649–669.
Levitt, JB. Kiper, Movshon. 1994. Receptive fields and functional architecture of macaque V2. J Neurophysiol. 71(6):2517–2542.
Levitt JB, Yoshioka T, Lund JS. 1995. Connections between the pulvinar complex and cytochrome oxidase-defined compartments in visual area V2 of macaque monkey. Exp Brain Res. 104(3):419–430.
Livingstone MS, Hubel DH. 1984a. Anatomy and physiology of a color system in the primate visual cortex. J Neurosci 4:309–356.
Livingstone MS, Hubel DH. 1984b. Specificity of intrinsic connections in primate primary visual cortex. J Neurosci. 4(11):2830–2835.
Livingstone MS, Hubel DH. 1987. Connections between layer 4B of area 17 and the thick cytochrome oxidase stripes of area 18 in the squirrel monkey. J Neurosci. 7(11):3371–3377.
Logothetis NK, Pauls J, Augath M, Trinath T, Oeltermann A. 2001. Neurophysiological investigation of the basis of the fMRI signal. Nature. V412:150–157.
Malach R, Tootell RB, Malonek D. 1994. Relationship between orientation domains, cytochrome oxidase stripes, and intrinsic horizontal connections in squirrel monkey area V2. Cereb Cortex. 4(2):151–165.
Malonek D, Grinvald A. 1996. Interactions between electrical activity and cortical microcirculation revealed by imaging spectroscopy: implications for functional brain mapping. Science. 272(5261):551–554.
Mazer JA, Vinje WE, McDermott J, Schiller PH, Gallant JL. 2002. Spatial frequency and orientation tuning dynamics in area V1. Proc Natl Acad Sci USA. 99(3):1645–1650.
Mehta AD, Ulbert I, Schroeder CE. 2000. Intermodal selective attention in monkeys. II: physiological mechanisms of modulation. Cereb Cortex. 10(4):359–370.
Merigan WH, Maunsell JH. 1993. How parallel are the primate visual pathways? Annu Rev Neurosci. 16:369–402.
Nealey TA, Maunsell JH. 1994. Magnocellular and parvocellular contributions to the responses of neurons in macaque striate cortex. J Neurosci. 14(4):2069–2079.
Norton TT, Casagrande VA, Irvin GE, Sesma MA, Petry HM. 1988. Contrast sensitivity functions of W-, X-, and Y-like relay cells in the lateral geniculate nucleus of the Bush Baby, *Galago crassicaudatus*. J Neurophysiol. 59:1639–1656.
Peterhans E, von der Heydt R. 1993. Functional organization of area V2 in the alert macaque. Eur J Neurosci. 5(5):509–524.
Peng X, Van Essen DC. 2005. Peaked encoding of relative luminance in macaque areas V1 and V2. J Neurophysiol. 93(3):1620–1632.
Ramsden BM, Hung CP, Roe AW. 2001. Real and illusory contour processing in area V1 of the primate: a cortical balancing act. Cereb Cortex. 11(7):648–665.
Roe AW, Lu HD. 2006. Functional organization of color domains in V1 and V2 of Macaque monkey revealed by optical imaging [VSS 2006 Abstract]. J Vis. 6(6):405a
Roe AW, Lu HD, Hung CP. 2005a. Cortical processing of a brightness illusion. Proc Natl Acad Sci USA. 102(10):3869–3874.
Roe AW, Fritsches K, Pettigrew JD. 2005b. Optical imaging of functional organization of V1 and V2 in marmoset visual cortex. Anat Rec A Discov Mol Cell Evol Biol. 287(2):1213–1225.
Roe AW, Ts'o DY. 1995. Visual topography in primate V2: multiple representation across functional stripes. J Neurosci. 15:3689–3715.
Roe AW, Ts'o DY. 1999. Specificity of color connectivity between primate V1 and V2. J Neurophysiol. 82(5):2719–2730.
Rossi AF, Rittenhouse CD, Paradiso MA. 1996. The representation of brightness in primary visual cortex. Science. 273:(5278)1104–1007.
Schmidt KF, Lowel S. 2006. Optical imaging in cat area 18: strabismus does not enhance the segregation of ocular dominance domains. Neuroimage. 29(2):439–445.
Shapley R, Perry VH. 1986. Cat and monkey retinal ganglion cells and their visual functional roles. Trends Neurosci. 9:229–235.
Shapley RM, Victor JD. 1978. The effect of contrast on the transfer properties of cat retinal ganglion cells. J Physiol. 285:275–298.
Shoham D, Hubener M, Schulze S, Grinvald A, Bonhoeffer T. 1997. Spatio-temporal frequency domains and their relation to cytochrome oxidase staining in cat visual cortex. Nature. 385(6616):529–533.
Shostak Y, Ding Y, Mavity-Hudson J, Casagrande VA. 2002. Cortical synaptic arrangements of the third visual pathway in three primate species: Macaca mulatta, Saimiri sciureus, and Aotus trivirgatus. J Neurosci. 22(7):2885–2893.
Sincich LC, Horton JC. 2002. Divided by cytochrome oxidase: a map of the projections from V1 to V2 in macaques. Science. 295:1734–1737.
Solomon SG, White AJ, Martin PR. 1999. Temporal contrast sensitivity in the lateral geniculate nucleus of a New World monkey, the marmoset Callithrix jacchus. J Physiol. 517:907–917.
Solomon SG, White AJ, Martin PR. 2002. Extraclassical receptive field properties of parvocellular, magnocellular, and koniocellular cells in the primate lateral geniculate nucleus. J Neurosci. 22(1):338–349.

Tootell RB, Hamilton SL. 1989. Functional anatomy of the second visual area (V2) in the macaque. J Neurosci. 9(8):2620–2644.
Tootell RB, Hamilton SL, Switkes E. 1988a. Functional anatomy of macaque striate cortex. III. Color. J Neurosci. 8(5):1569–1593.
Tootell RB, Hamilton SL, Switkes E. 1988b. Functional anatomy of macaque striate cortex. IV. Contrast and magno-parvo streams. J Neurosci. 8(5):1594–1609.
Ts'o DY, Roe AW, Gilbert CD. 2001. A hierarchy of the functional organization for color, form and disparity in primate visual area V2. Vision Res. 41(10–11):1333–1349.
Ts'o Frostig RD, Lieke EE, Grinvald A. 1990. Functional organization of primate visual cortex revealed by high resolution optical imaging. Science. 249(4967):417–420.
Xiao Y, Wang Y, Felleman DJ. 2003. A spatially organized representation of colour in macaque cortical area V2. Nature. 421(6922):535–539.
Xu X, Bosking W, Sary G, Stefansic J, Shima D, Casagrande V. 2004. Functional organization of visual cortex in the owl monkey. J Neurosci. 24(28):6237–6247.
Xu X, Bosking WH, White LE, Fitzpatrick D, Casagrande VA. 2005. Functional organization of visual cortex in the prosimian bush baby revealed by optical imaging of intrinsic signals. J Neurophysiol. 94(4):2748–2762.
Yabuta NH, Callaway EM. 1998. Functional streams and local connections of layer 4C neurons in primary visual cortex of the macaque monkey. J Neurosci. 18(22):9489–9499.
Zhan C, Baker CL. 2006. Boundary cue invariance in cortical orientation maps. Cereb Cortex. 16(6):896–906.
Zhan C, Ledgeway T, Baker CL. 2005. Contrast response in visual cortex: quantitative assessment with intrinsic optical signal imaging and neural firing. Neuroimage. 26(2):330–346.